

DIRECT POWER CONTROL OF GRID CONNECTED WOUND ROTOR INDUCTION GENERATOR

A DISSERTATION

*Submitted in partial fulfillment of the
requirements for the award of the degree*

of

MASTER OF TECHNOLOGY

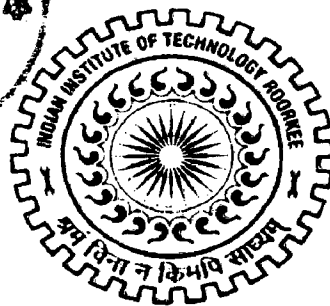
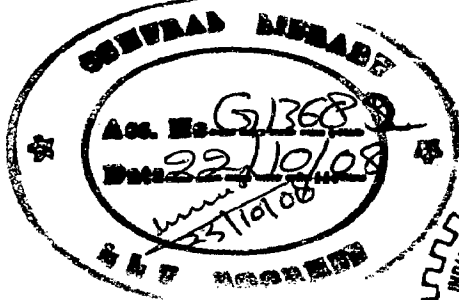
in

ELECTRICAL ENGINEERING

(With Specialization in Power Apparatus & Electric Drives)

By

G/13682 **VAVILAPALLI SRIDHAR**



**DEPARTMENT OF ELECTRICAL ENGINEERING
INDIAN INSTITUTE OF TECHNOLOGY ROORKEE
ROORKEE - 247 667 (INDIA)**

JUNE 2008

CANDIDATE'S DECLARATION

I hereby declare that the work which is being presented in this dissertation entitled, "**Direct Power Control Of Grid Connected Wound Rotor Induction Generator**" submitted in the partial fulfillment of the requirements for the award of the degree "**Master of Technology**" with specialization in **Power Apparatus And Electric Drives**, to the **Department of Electrical Engineering, IIT Roorkee**, Roorkee is an authentic record of my own work carried out during the period from August 2007 to June 2008 under the supervision of **Mr. Y.P.Singh**, Asst.Professor and **Dr. S Ghatak Choudhuri**, Asst.Professor, Department of Electrical Engineering, IIT Roorkee, Roorkee.

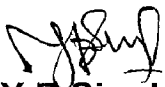
The matters embodied in this report have not been submitted by me for the award of any other degree or diploma.

Date: June 2008

Place: Roorkee

(VAVILAPALLI SRIDHAR)

This is to certify that above statement made by candidates is correct to the best of my knowledge.



(Mr. Y.P.Singh)

Asst.Professor,
Electrical Engineering Department,
I.I.T.Roorkee.



(Dr. S Ghatak Choudhuri)

Asst.Professor,
Electrical Engineering Department,
I.I.T.Roorkee.

ABSTRACT

Direct power control which is a rotor side control of a doubly fed induction generator by which decoupled control of stator active and reactive power can be obtained is presented. It is based on the measurement of active and reactive power on the grid side where voltages and currents are alternating at fixed frequency. The active and reactive powers are made to track references using hysteresis controllers. The measurements are taken on stator side and the control is made on rotor side. This control system eliminates the need for rotor position sensing and gives an excellent dynamic performance as shown by simulation results for a variable speed constant frequency induction generator system. The system can be operated below, above and at synchronous speeds.

The operation of the doubly fed induction generator (DFIG) system is explained. The power control by rotor current injection is explained by the phasor diagrams. The controlling scheme is explained and the modeling of the complete system is done in MATLAB-SIMULINK.

The dynamic performance of the system is observed and compared with vector control scheme. The response of the stator and rotor currents, power factor, stator and rotor powers for different values of reference active and reactive powers are shown by the simulation results.

The performance of this control technique in wind power applications is observed. Optimum power control and pitch angle control for wind turbine is proposed and the response of generator speed, pitch angle, optimum power, turbine torque, stator current, stator and rotor powers for different wind speeds are shown by simulation results. The direction of stator and rotor power flow is explained with simulation results.

CANDIDATE'S DECLARATION

I hereby declare that the work which is being presented in this dissertation entitled, "**Direct Power Control Of Grid Connected Wound Rotor Induction Generator**" submitted in the partial fulfillment of the requirements for the award of the degree "**Master of Technology**" with specialization in **Power Apparatus And Electric Drives**, to the **Department of Electrical Engineering, IIT Roorkee**, Roorkee is an authentic record of my own work carried out during the period from August 2007 to June 2008 under the supervision of **Mr. Y.P.Singh**, Asst.Professor and **Dr. S Ghatak Choudhuri**, Asst.Professor, Department of Electrical Engineering, IIT Roorkee, Roorkee.

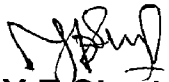
The matters embodied in this report have not been submitted by me for the award of any other degree or diploma.

Date: June 2008

Place: Roorkee


(VAVILAPALLI SRIDHAR)

This is to certify that above statement made by candidates is correct to the best of my knowledge.



(Mr. Y.P.Singh)

Asst.Professor,
Electrical Engineering Department,
I.I.T.Roorkee.



(Dr. S Ghatak Choudhuri)

Asst.Professor,
Electrical Engineering Department,
I.I.T.Roorkee.

ACKNOWLEDGEMENT

I would like to give my sincere gratitude to Shri.Y.P.Singh, Asst. professor, and Dr. S Ghatak choudhuri, Asst. Professor, Electrical Engineering Department, Indian Institute of Technology, Roorkee, for pointed me to the topic Direct power control of grid connected wound rotor induction generator, as well as providing me all the necessary guidance and the inspirational support throughout the Dissertation.

My heartfelt gratitude and indebtedness goes to all the staff of Power apparatus & Electric drives group who, with their encouraging and caring words, constructive criticism and suggestions have contributed directly or indirectly in a significant way towards completion of this Dissertation.

I convey my deep sense of gratitude to the Head of Electrical Engineering Department, who directly or indirectly helped me during the work.

I am indebted to all my classmates from Power apparatus & Electric drives group for taking interest in discussing my problems and encouraging me.

VAVILAPALLI SRIDHAR

M.Tech (Power apparatus & Electric drives)

ABSTRACT

Direct power control which is a rotor side control of a doubly fed induction generator by which decoupled control of stator active and reactive power can be obtained is presented. It is based on the measurement of active and reactive power on the grid side where voltages and currents are alternating at fixed frequency. The active and reactive powers are made to track references using hysteresis controllers. The measurements are taken on stator side and the control is made on rotor side. This control system eliminates the need for rotor position sensing and gives an excellent dynamic performance as shown by simulation results for a variable speed constant frequency induction generator system. The system can be operated below, above and at synchronous speeds.

The operation of the doubly fed induction generator (DFIG) system is explained. The power control by rotor current injection is explained by the phasor diagrams. The controlling scheme is explained and the modeling of the complete system is done in MATLAB-SIMULINK.

The dynamic performance of the system is observed and compared with vector control scheme. The response of the stator and rotor currents, power factor, stator and rotor powers for different values of reference active and reactive powers are shown by the simulation results.

The performance of this control technique in wind power applications is observed. Optimum power control and pitch angle control for wind turbine is proposed and the response of generator speed, pitch angle, optimum power, turbine torque, stator current, stator and rotor powers for different wind speeds are shown by simulation results. The direction of stator and rotor power flow is explained with simulation results.

LIST OF FIGURES

Fig. No	Figure Name	Page No
1.1	constant speed constant frequency WECS using squirrel cage machine	2
1.2	Variable Speed Constant Frequency WECS using squirrel cage machine	2
1.3	Variable speed constant frequency WECS using DFIG	3
2.1	schematic diagram of the DFIG system	7
2.2	Power flow diagram of a DFIG	9
2.3	Approximate equivalent circuit and Phasor diagram	9
2.4	Phasor diagram showing variations in rotor flux with change rotor current	11
2.5	Simulink model of doubly fed induction generator	13
2.6	Simulink model of the mechanical system	13
2.7	Front end converter	14
2.8	Voltage control loop of front end converter	15
2.9	Simulink model of Front end converter	15
2.10	Mathematical model of Machine side converter	16
3.1	Schematic diagram of Direct power control of DFIG	17
3.2	(a) Orientation of the rotor winding in space with respect to which the voltage space phasors are drawn (b) Voltage space phasors.	18
3.3	Flux vectors generating mode	19
3.4	Simulink model of direct power control scheme	22
3.5	Simulink model of Hysteresis controllers	23
3.6	Simulink model for producing conditions	24
3.7	Simulink model of Pulse generation	25
3.8	Simulink model of sector identification	26

3.9	Modeling of the direct power control of DFIG system in simulink	26
3.10	Response of stator active power for step change in reference active power	27
3.11	Response of stator reactive power for step change in reference reactive power	27
3.12	Response of P_s for different values of P_s^*	28
3.13	Response of Q_s for different values of Q_s^*	29
3.14	Response of Stator current for different values of P_s and Q_s	30
3.15	V_s and I_s when Q_s is Zero	31
3.16	V_s and I_s when $Q_s=1$ and $P_s=0$	31
3.17	V_s and I_s when $Q_s=1$ and $P_s=1$	32
3.18	Response of active power with d-axis component of current	33
3.19	Response of reactive power with q-axis component of current	34
3.20	modeling of vector control of DFIG	35
3.21	PI controllers used in tracking of active and reactive powers	36
3.22	Vector control scheme for machine side converter	36
3.23	Response of active and reactive power for a step change in reference powers	37
4.1	Simulink model of wind turbine with optimum power control	38
4.2	C_p - λ characteristics	40
4.3	Simulink model of the wind turbine	41
4.4	Turbine power characteristics and Tracking characteristics	42
4.5	Optimum stator power curve	43
4.6	The Simulink model of the wind turbine with pitch angle control and optimum power control	44
5.1	Wind power generation by DFIG incorporated with DPC	45

5.2	Response of generator speed, mechanical torque and optimum power with change in wind velocity	46
5.3	Response of speed and pitch angle with change in wind speed	47
5.4	Stator active power and Optimum power	48
5.5	Stator active power, reactive power and current	49
5.6	Change in Rotor active power with speed	50
5.7	pitch angle and generator speed at 2.5 p.u. wind speed	51
5.8	pitch angle and generator speed at 3 p.u. Wind speed	52
5.9	pitch angle and generator speed at 3.5 p.u. wind speed	52
5.10	pitch angle and generator speed at 3.67 p.u. wind speed	53
5.11	pitch angle and generator speed at 3.75 p.u. wind speed	53
5.12	pitch angle and generator speed at 4 p.u. wind speed	54
5.13	pitch angle and generator speed at 4.5 p.u. wind speed	54
5.14	Generator efficiency versus wind speed	55

CONTENTS

	Page no
CANDIDATE DECLARATION	i
ACKNOWLEDGEMENT	ii
ABSTARCT	iii
LIST OF FIGURES	iv
CHAPTER 1: INTRODUCTION	1- 6
1.1 Introduction	1
1.2 Advantages of DFIG	4
1.3 Literature Review	5
CHAPTER 2: DFIG SYSTEM OVERVIEW	7 - 16
2.1 Introduction	7
2.2 Direction of Power flow in DFIG	8
2.3 Equivalent circuit of DFIG	9
2.4 Concept of independent control of Active and Reactive power	10
2.5 Mathematical modeling of the DFIG	12
2.6 Modeling of Front end converter	14
2.7 Modeling of Machine side converter	16
CHAPTER 3: DIRECT POWER CONTROL OF DFIG	17 - 37
3.1 Introduction	17
3.2 Concept of Direct Power Control	18
3.3 Implementation of Direct power control Algorithm in Simulink	22
3.4 Simulation Results	27
3.5 Comparison of DPC with vector control	35

CHAPTER 4: WIND TURBINE	38 - 44
4.1 Introduction	38
4.2 Wind Turbine modeling	38
4.3 Optimum power control	41
4.4 Pitch angle control	43
CHAPTER 5: DPC OF DFIG IN WIND POWER APPLICATIONS	45 - 56
5.1 Introduction	45
5.2 Simulation Results	46
CHAPTER 6: CONCLUSIONS	57
REFERENCES	58 – 59
APPENDIX	60

1. Introduction

1.1. Introduction:

The induction machine which is driven by a turbine works as a generator with stator connected to the grid and a rotor fed by back to back connected PWM converters with a common dc link. The machine rotor speed changes in a limited range. A machine control system controls two quantities: active and reactive powers. These both quantities are controlled by the rotor currents of such a magnitude and frequency that makes it possible to maintain the reference values of powers. The main application of this power control of DFIG is in wind power generation.

A Wind Energy Conversion System (WECS) can vary in size from a few hundred kilowatts to several megawatts. The size of the WECS largely determines the choice of the generator and converter system. Asynchronous generators are more common with systems up to 2MW, beyond which direct-driven permanent magnet synchronous machines are preferred.

Conventionally grid-connected cage rotor induction machines are used as wind generators at medium power level. When connected to the constant frequency network, the induction generator runs at near synchronous speed drawing the magnetizing current from the mains, thereby resulting in constant speed constant frequency (CSCF) operation [12].

Constant speed constant frequency WECS using cage rotor induction machine

Constant speed constant frequency (CSCF) WECS using cage rotor induction generators shown in Fig: 1.1 are most widely used because of their design simplicity and low cost.

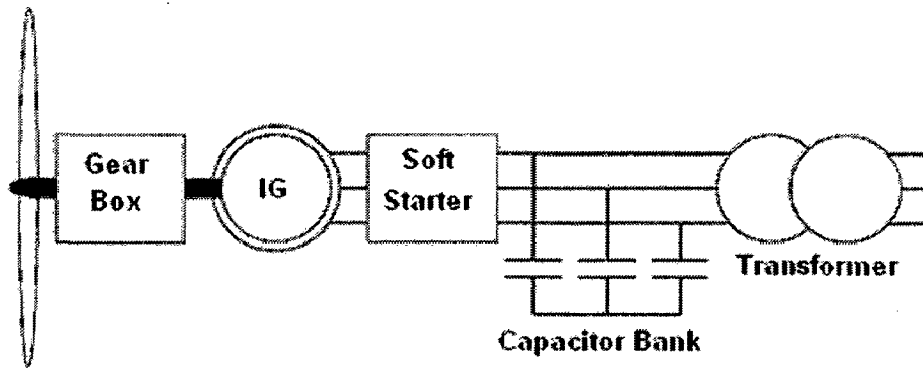


Fig 1.1: constant speed constant frequency WECS using squirrel cage machine [14]

A fixed speed system, even though more simple and reliable, severely limits the energy output of a wind turbine and the speed of wind is also fluctuating in nature. However the power capture due to fluctuating wind speed can be substantially improved if there is flexibility in varying the shaft speed to maximize power capture with fluctuating wind velocities. Therefore, WECS is a classic example of a variable speed constant frequency (VSCF) system [14].

Variable speed constant frequency WECS using cage rotor induction machine

Variable speed systems with cage rotor induction generators Fig. 1.2 are also commercially available where energy output can be substantially improved and unity power factor operation is possible

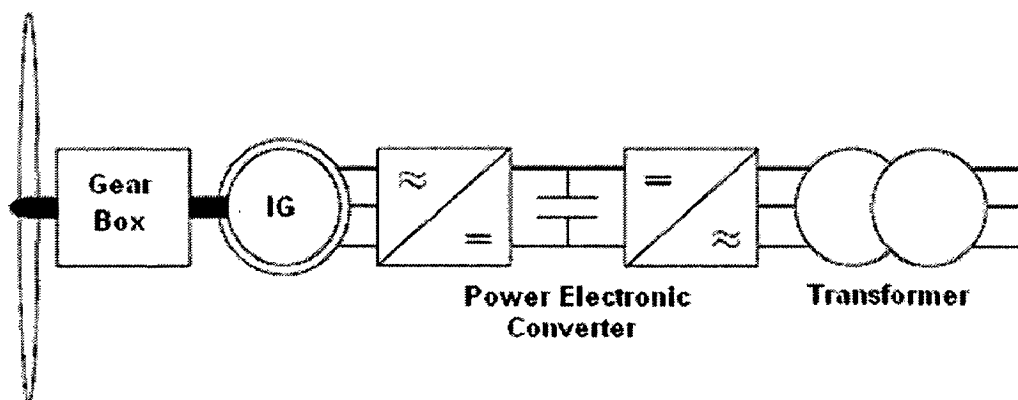


Fig 1.2: Variable Speed Constant Frequency WECS using squirrel cage machine [14]

Here in this system the converters ratings are equals to the stator power rating as these converters have to carry the rated power of the machine. So cost of converters is high. So in such variable speed constant frequency (VSCF) application rotor side control of grid-connected wound rotor induction machine is an attractive solution. Such an arrangement provides flexibility of operation in sub-synchronous and super-synchronous speeds both in the generating and motoring modes. The rating of the power converters used in the rotor circuit is substantially lower than the machine rating and is decided by the range of operating speed [14].

Variable speed constant frequency WECS using doubly fed induction machine

In this type of system, the stator is directly connected to the three phase grid and the rotor is supplied by two back-to-back PWM converters as shown in Fig. 1.3. Of the two converters, the function of the line side converter is to regulate the dc bus voltage and act as unity power factor interface to the grid for either direction of power flow. The machine side converter has to control the active and reactive powers. The present work is concerned with the control of the machine side converter.

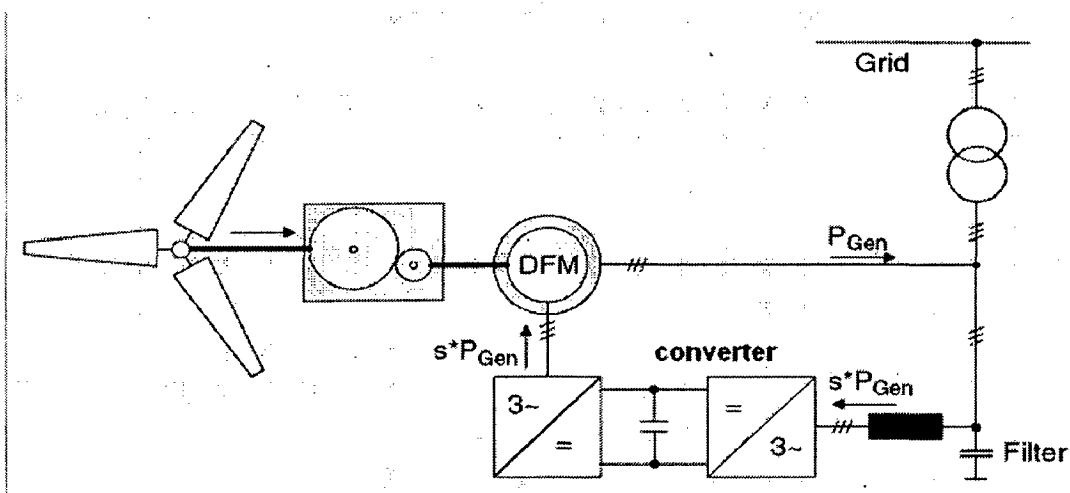


Fig 1.3: Variable speed constant frequency WECS using DFIG [14]

With a suitable integrated approach toward design of a WECS, use of a slip-ring induction generator is economically competitive, when compared to a cage rotor induction machine. The higher cost of the machine due to the slip rings is compensated by a reduction in the size of the power converters. The generator rating can also be reduced compared to other singly fed machines [6].

It is possible to operate the system up to higher wind velocities. The voltage rating of the power devices and dc bus capacitor is substantially reduced. The size of the line side inductor also decreases. So a variable speed system using wound rotor induction machine is superior because of higher energy output, lower rating hence, lower cost of converters [14].

1.2 Advantages of DFIG:

This DFIG offers the following advantages over other schemes of WECS

- (1) Reduced inverter cost, because inverter rating is typically 25% of total system power, while the speed range of the ASG is 33% around the synchronous speed
- (2) Reduced cost of the inverter filters and EMI filters, because filters are rated for 0.25 p.u. of total system power.
- (3) Improved system efficiency; approximately 2-3% efficiency improvement can be obtained.

Power-factor control can be implemented at lower cost, because the DFIG system (four-quadrant converter and induction machine) basically operates similar to a synchronous generator. The converter has to provide only excitation energy. The DFIG with a four -quadrant converter in the rotor circuit enables decoupled control of active and reactive power of the generator [6].

1.3 Literature Review:

Cardici .I and Ermis M presented a paper on the steady state performance of Double-output induction generator operating at sub-synchronous and super-synchronous speeds [3].

E. Bogalecka investigated on Power control of a double fed induction generator without position sensors. The proposed Control system controls the active and the reactive powers by means of the rotor currents. The control system produces directly the rotor currents frequency without rotor position measurement and coordinates transformations. An angle controller is introduced. This controls the angle between two vectors. Possibilities of the angle real value calculations are presented [4].

Longya Xu and Wei Cheng studied the Torque and Reactive Power Control of a Doubly Fed Induction Machine by Position Sensor less Scheme. The critical issues related to the torque angle estimation and control for a doubly excited induction machine is discussed [5].

R.Pena, J.C.Clare and G.M.Asher investigated on doubly fed induction generator using back-to-back PWM converters and its application to variable speed wind-energy generation. In this a vector-control scheme for the supply-side PWM converter and the rotor-connected converters is presented [6].

C. Knowles-Spittle, N.D.Maclsaac and B. A. T. Al Zahawi studied the Analysis of 1.4 MW Static Scherbius drive with Sinusoidal Current Converters In Rotor Circuit. A rigorous analysis of the Static Scherbius Drive with two IGBT sinusoidal current converters in the rotor circuit is presented. The analysis is based on a hybrid dq model in which stator variables only are transformed on to a frame of reference stationary with respect to the rotor [8].

R. Datta and V.T.Ranganathan presented a scheme on field-oriented control of a doubly-fed wound rotor induction machine without shaft position sensors. Instead of using dynamic angle controllers for rotor position estimation, a direct method based on simple transformations is proposed. Decoupled control of active and reactive powers for the rotor side and front-end converters under transient and steady-state

conditions is demonstrated. The presented scheme is a viable alternative to cage-rotor induction generators for variable-speed wind energy applications [9].

S. Muller, M. Deicke and R.W. De Doncker presented paper on the performance of Adjustable Speed Generators for Wind Turbines based on Doubly-fed Induction Machines. The doubly-fed induction generator (DFIG) system is investigated as a viable alternative to adjust speed over a wide range while keeping cost of the power converters minimal [11].

Rajib Datta and V. T. Ranganathan presented an algorithm for Direct Power Control of Grid- Connected Wound Rotor Induction Machine without Rotor Position Sensors. The active and reactive powers are made to track references using hysteresis controllers. The method eliminates the need for rotor position sensing and gives excellent dynamic performance [12].

Zbigniew Krzeminski investigated a Sensor less Multiscalar Control of Double Fed Machine For Wind Power Generators. In this Nonlinear feedback transforms the system into two independent linear subsystems. Estimation of variables including the rotor position has been applied to the system. The active and reactive powers of the stator are controlled using PI controllers. With this control scheme there is no mutual dependence of transients of the active power on reactive power are observed and the system is stable [13].

Debiprasad Panda, Thomas .A.Lipo presented a paper on A double side converter fed wound rotor induction machine control for a wind energy application. In order to reduce the cost of a wind generator system, a new configuration using half controlled converters for both the stator and rotor circuit as well as for the line side is proposed. The proposed controller reduces the required KVA rating of both machine side and line side converters, improves the efficiency of the wind generator, helps operating over a wide speed range and supports near unity power factor interface with the grid [18].

DFIG System overview

2.1 Introduction:

In a doubly-fed wound rotor machine, the control can be realized either from the stator side or the rotor side or from both the sides. The machine can be controlled as a generator in both the sub-synchronous and super-synchronous operating modes.

Since the rotor side control strategy becomes advantageous within a limited slip range, the operating region is spread out on both sides of the synchronous speed ω_s , implying both sub-synchronous and super-synchronous modes of operation.

The stator of the wound rotor machine is connected to the balanced three phase grid and the rotor side is fed via two back-to-back IGBT voltage source inverters with a common dc bus as shown in fig 2.1. Since the speed range is restricted, the slip induced voltage is only a fraction of the grid voltage. Therefore, the dc bus voltage is kept relatively low. This necessitates a step-down transformer at the line-side interface.

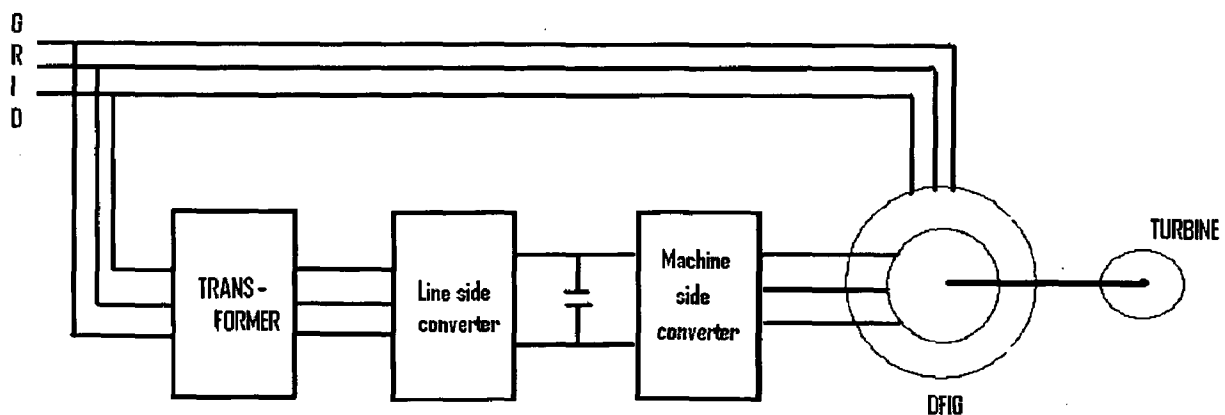


Fig 2.1: schematic diagram of the DFIG system

The front-end converter (FEC) controls the power flow between the dc bus and the ac side. It has the same three phase bridge topology that of the rotor side

converter. This back-to-back arrangement of two PWM converters with a common dc bus makes the system extremely flexible in terms of control of active and reactive power flow. The machine can now be operated in sub-synchronous and super-synchronous speeds because the rotor circuit is capable of sourcing and sinking the slip power. Even though the active power flow is proportional to the slip, the reactive power flow can be independently controlled for the machine side and line side converters; hence the overall system power factor can be kept at unity under varying conditions of load / input [6].

The rating of the power converters used in the rotor circuit is substantially lower than the machine rating and is decided by the range of operating speed. Of the two converters, the function of the line side converter is to regulate the dc bus voltage and act as unity power factor interface to the grid for either direction of power flow. The machine side converter has to control the torque and flux of the machine or alternatively the active and reactive powers [12].

2.2 Direction of Power flow in DFIG:

In generating mode the shaft is driven by the Turbine and the mechanical energy is converted into electrical energy and pumped out of the stator with negative torque. The mechanical power input to the shaft $P_m = (1-s) P_s$.

The direction of power flow in the case of Rotor side control of doubly fed induction generator is explained by the fig 2.2 shown below: Depending on the operating modes, the power flow varies in the stator and the rotor winding of the machine and the detail power flow diagram for different operating modes are given in Fig 2.2.

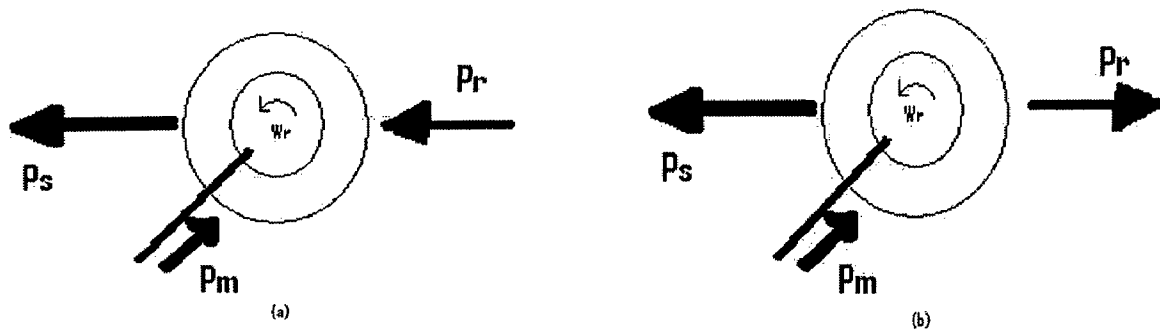


Fig 2.2: Power flow diagram of a doubly-fed wound rotor induction machine for (a) Sub-synchronous generating mode (b) Super-synchronous generating mode [2]

In the Sub-synchronous speed range slip S is positive and stator power is P_s correspondingly slip power SP_s is fed to the rotor. In Super-Synchronous Generating mode P_s remains constant but additional mechanical power input is reflected as slip power output [2].

2.3 Equivalent circuit of DFIG:

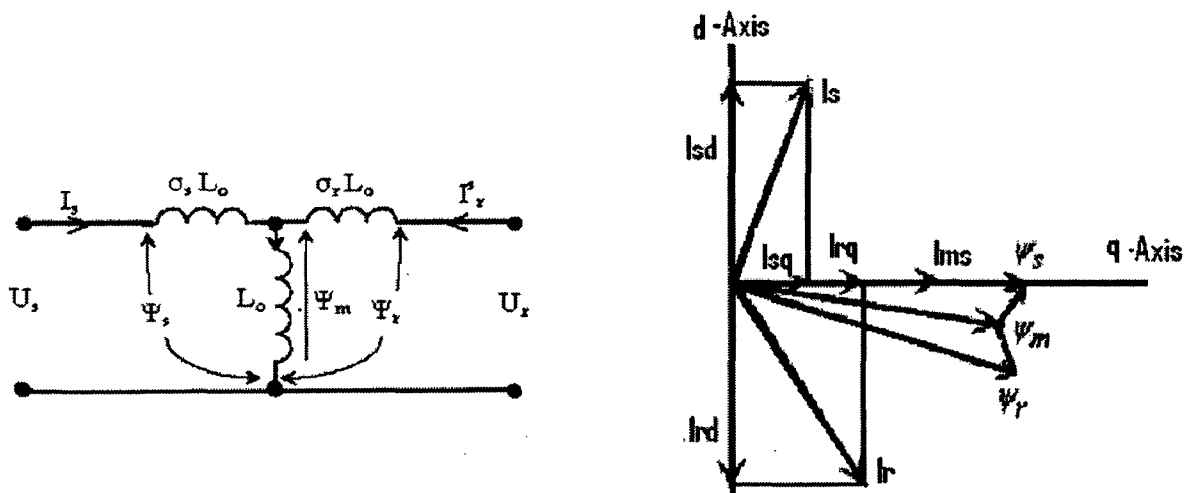


Fig 2.3: Approximate equivalent circuit and Phasor diagram [9]

Assuming negligible stator resistance drop the stator flux Ψ_s , and hence the stator flux magnetizing current I_{ms} remain constant in magnitude lagging the stator voltage vector by 90° . The magnitude of I_{ms} can be defined as

$$I_{ms} = (1 + \sigma_s) I_{sq} + I_{rq} \dots\dots\dots (2.1)$$

Since control is exercised on the rotor side an injection of positive I_{rq} will naturally result in lesser value of I_{sq} being drawn from the stator terminals leading to an improvement in the stator power factor

In the d-axis

$$0 = (1 + \sigma_s) I_{sd} + I_{rd} \dots\dots\dots (2.2)$$

The magnitude of I_{sd} being directly proportional to I_{rd} . The machine can be looked upon as a current transformer as far as the active power flow in the stator and the rotor are concerned. In the phasor diagram an injection of positive I_{rd} implies that I_{sd} is negative indicating active power flow into the grid at the stator terminals [9].

2.4 Concept of independent control of active and reactive power:

The effect of injection of these rotor currents on the air-gap and rotor fluxes can be derived by subtracting and adding the respective leakage fluxes. The variation of the rotor flux with variations in the active and reactive power demand is shown in Fig. 2.4(a) and (b). In Fig. 2.4(a) $I_{rq}=0$, i.e., the reactive power is fed completely from the stator side. Under this condition if I_{rd} is varied from 0 to full load, the locus of Ψ_r varies along A–B which indicates a predominant change in angle δ between Ψ_s and Ψ_r , whereas the magnitude of Ψ_r does not change appreciably. In other words, a change in the angle δ would definitely result in a change in the active power handled by the stator in a predictable fashion.

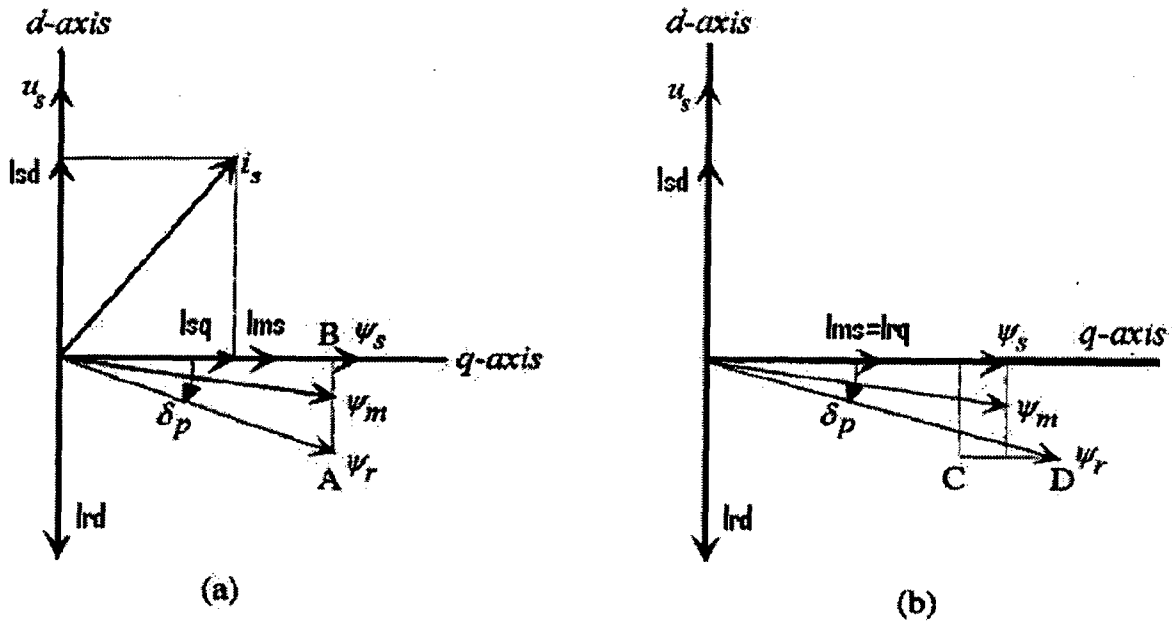


Fig 2.4: Phasor diagram showing variations in rotor flux with change in rotor current.

In Fig. 2.4(b) the stator active power demand is maintained constant so that I_{rd} is constant and I_{rq} is varied from 0 to the rated value. Here the locus of Ψ_r varies along C–D, resulting in a predominant change in magnitude of Ψ_r , whereas the variation of δ is small. Therefore, the reactive power drawn from the grid by the stator can be reduced by increasing the magnitude of the rotor flux and vice-versa. It may be noted that the phasor diagrams as indicated in Fig. 2.4(a) and (b) remain same irrespective of the reference frame; the frequency of the phasors merely changes from one reference frame to the other. It can be concluded from the above discussion that

- i) The stator active power can be controlled by controlling the angular position of the Rotor flux vector.
- ii) The stator reactive power can be controlled by controlling the magnitude of the Rotor flux vector.

These two basic notions are used to determine the instantaneous switching state of the rotor side converter to control the active and reactive power [12].

2.5 Mathematical modeling of the DFIG:

The induction machine is modeled in vectorized form. The mechanical system is modeled as two inertias coupled by means of a flexible shaft. The whole system is described by parameters expressed in per unit [1].

Stator and Rotor Voltages of an Induction machine are

$$\begin{bmatrix} V_{sd} \\ V_{sq} \end{bmatrix} = \begin{bmatrix} I_{sd} \\ I_{sq} \end{bmatrix} R_s + \frac{1}{W_0} \frac{d}{dt} \begin{bmatrix} \phi_{sd} \\ \phi_{sq} \end{bmatrix} + W_k \begin{bmatrix} -\phi_{sq} \\ \phi_{sd} \end{bmatrix}$$

$$\begin{bmatrix} V_{rd} \\ V_{rq} \end{bmatrix} = \begin{bmatrix} I_{rd} \\ I_{rq} \end{bmatrix} R_r + \frac{1}{W_0} \frac{d}{dt} \begin{bmatrix} \phi_{rd} \\ \phi_{rq} \end{bmatrix} + (W_k - W_m) \begin{bmatrix} -\phi_{rq} \\ \phi_{rd} \end{bmatrix} \dots\dots\dots (2.3)$$

In the above equation

$W_k = W_s$ (synchronous speed) in rotating dq reference frame

$W_k = W_m$ (Rotor speed) in rotor reference frame

$W_k = 0$ in stator reference frame

Flux linkages are as given below

$$\begin{aligned} \phi_s &= L_s I_s + L_m I_r \\ \phi_r &= L_r I_r + L_m I_s \end{aligned} \dots\dots\dots (2.4)$$

From the above equations of flux linkages stator and rotor currents are

$$\begin{aligned} I_s &= \frac{\phi_s (L_r + L_m) - \phi_r (L_m)}{(L_s L_r + L_s L_m + L_m L_r)} \\ I_r &= \frac{\phi_r (L_s + L_m) - \phi_s (L_m)}{(L_s L_r + L_s L_m + L_m L_r)} \end{aligned} \dots\dots\dots (2.5)$$

Electro magnetic Torque

$$T_e = \phi_{ds} I_{qs} - \phi_{qs} I_{ds} \dots\dots\dots (2.6)$$

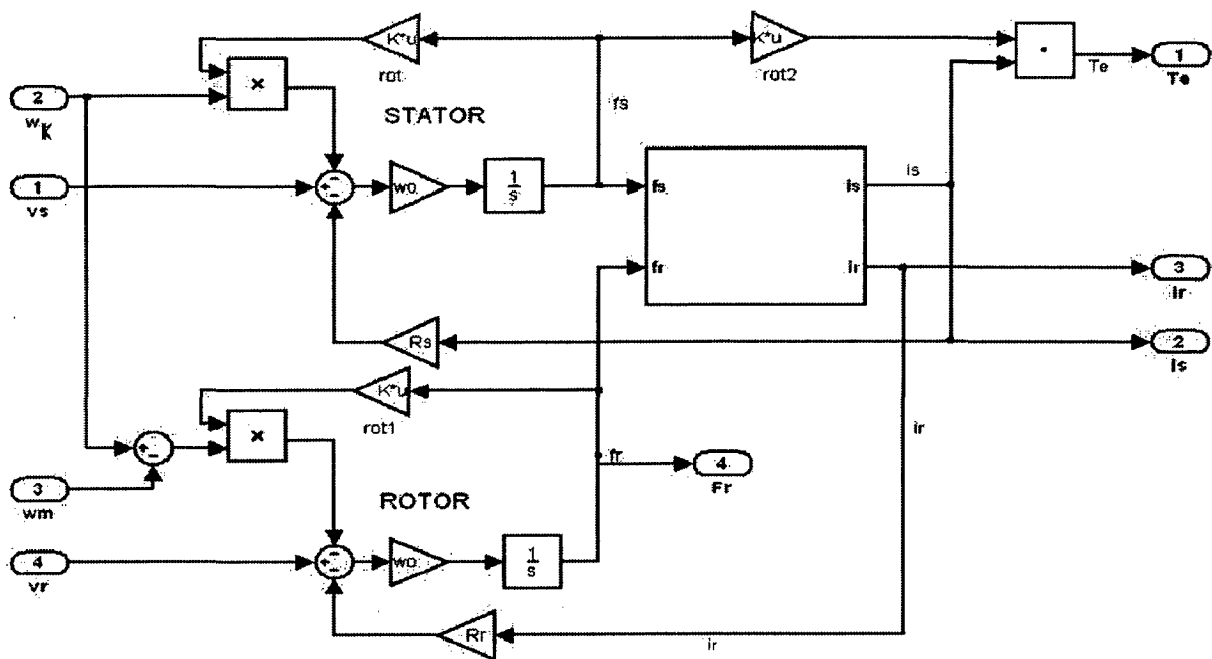


Fig 2.5: Simulink model of doubly fed induction generator

The mechanical system is modeled as two inertias coupled by means of a flexible shaft. Relation between generator speed, Electro magnetic torque and Turbine torque is as below

$$T_e = 2H \frac{d}{dt} W_m + B_m W_m + T_w \quad \dots \dots \dots (2.7)$$

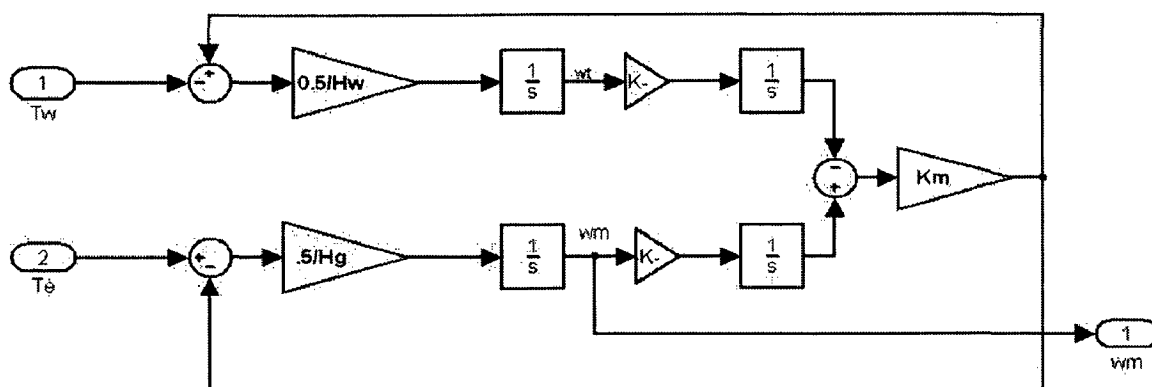


Fig 2.6: Simulink model of the mechanical system

2.6 Front end converter modeling:

The objective of the supply-side converter is to keep the DC-link voltage constant regardless of the magnitude and direction of the rotor power.

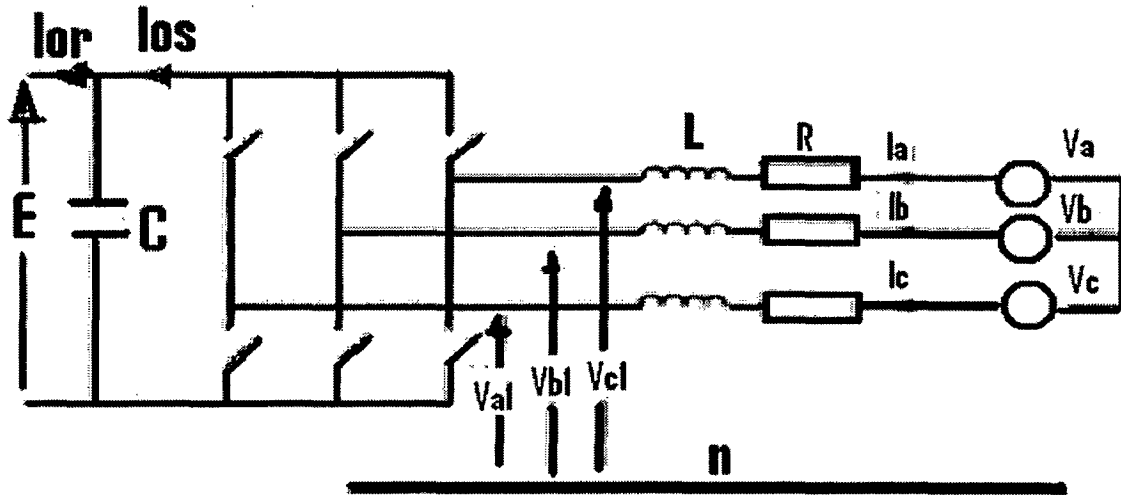


Fig 2.7: Front end converter [6]

The voltage equations is

$$\begin{bmatrix} V_a \\ V_b \\ V_c \end{bmatrix} = R^* \begin{bmatrix} I_a \\ I_b \\ I_c \end{bmatrix} + L \frac{d}{dt} \begin{bmatrix} I_a \\ I_b \\ I_c \end{bmatrix} + \begin{bmatrix} V_{a1} \\ V_{b1} \\ V_{c1} \end{bmatrix} \quad \dots\dots\dots (2.8)$$

Where L and R are the line inductance and resistance respectively. Using the transformations of the eqn. 2 is transformed into a dq reference frame rotating at ω_e

$$\begin{aligned} V_d &= RI_d + L \frac{dI_d}{dt} - \omega_e LI_q + V_{d1} \\ V_q &= RI_q + L \frac{dI_q}{dt} + \omega_e LI_d + V_{q1} \end{aligned} \quad \dots\dots\dots (2.9)$$

Aligning the d-axis of the reference frame along the stator-voltage position V_q is zero and since the amplitude of the supply voltage is constant V_d is constant. The active and reactive power will be proportional to I_d and I_q respectively [4].

Neglecting harmonics due to switching and the losses in the inductor resistance and converter, we have

$$EI_{os} = 3V_d I_d$$

$$V_d = \frac{m_1}{2\sqrt{2}} E$$

$$I_{os} = \frac{3}{2\sqrt{2}} m_1 I_d$$

$$C \frac{dE}{dt} = I_{os} - I_{or} \quad \dots\dots\dots (2.10)$$

It is seen that the DC-link voltage can be controlled via I_d .

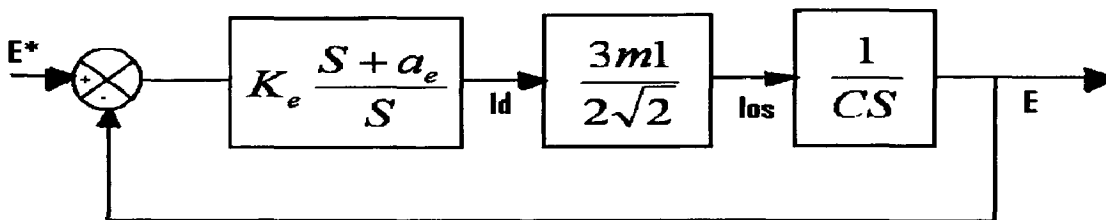


Fig 2.8: Voltage control loop of front end converter [6]

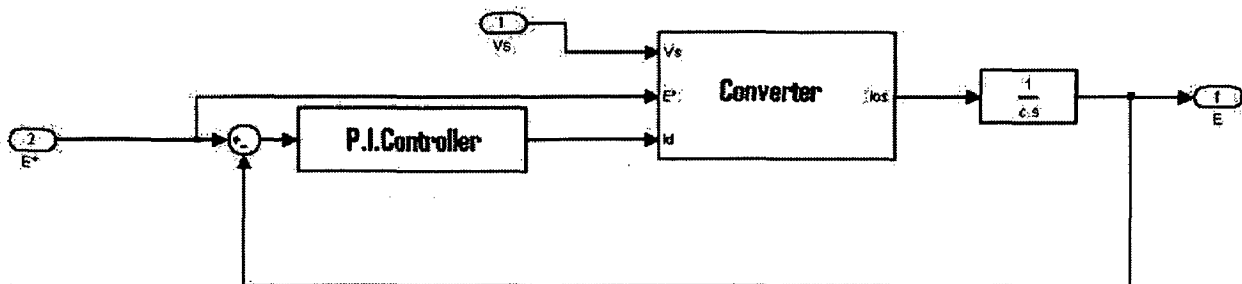


Fig 2.9: Simulink model of Front end converter

2.7 Machine side converter Modeling:

The rotor side converter has the same three phase bridge topology almost identical to that of the front-end converter (FEC).

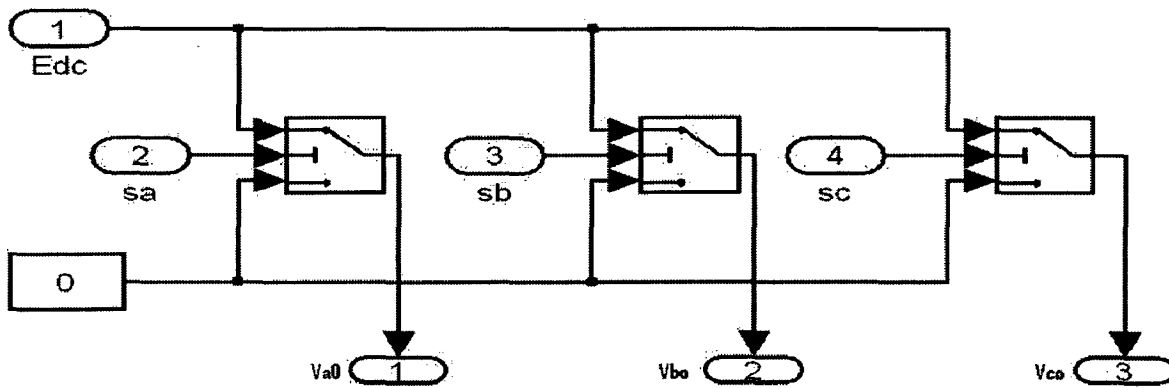


Fig 2.10: Mathematical model of Machine side converter

The line voltages are obtained by the following equation

$$\begin{bmatrix} Va \\ Vb \\ Vc \end{bmatrix} = \frac{1}{3} \begin{bmatrix} 2 & -1 & -1 \\ -1 & 2 & -1 \\ -1 & -1 & 2 \end{bmatrix} * \begin{bmatrix} Va0 \\ Vb0 \\ Vc0 \end{bmatrix} \dots\dots\dots (2.11)$$

Where Va, Vb, Vc are line voltages and $Va0, Vb0, Vc0$ are phase voltages

The machine side converter is controlled to control the active and reactive power of the machine. In the next chapter direct power control algorithm for machine side converter is explained.

Direct power control of DFIG

3.1 Introduction:

The conventional approach for independent control of active and reactive powers handled by the machine is stator flux oriented vector control with rotor position sensors. The performance of the system in this case depends on the accuracy of computation of the stator flux and the accuracy of the rotor position information derived from the position encoder. Alignment of the position sensor is moreover, difficult in a doubly-fed wound rotor machine.

An algorithm developed for independent control of active and reactive powers with high dynamic response is described in this section. The instantaneous switching state of the rotor side converter is determined based on the active and reactive powers measured in the stator circuit. Measurements are carried out at one terminal of the machine whereas the switching action is carried out at another terminal. Here the directly-controlled quantities are the stator active and reactive powers; hence the algorithm is referred as direct power control. It can be applied to VSCF applications like wind power generation [12].

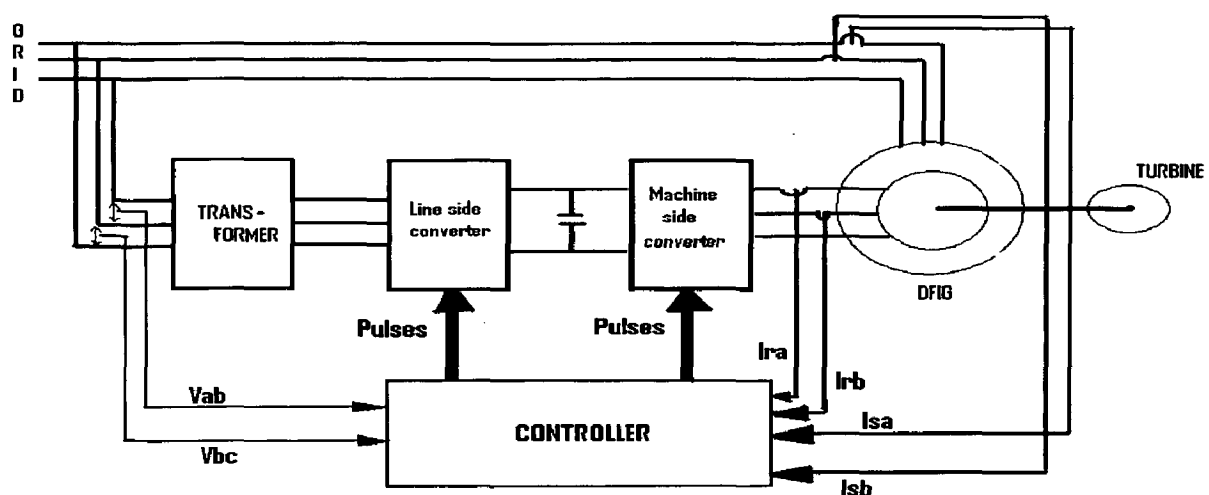


Fig 3.1: Schematic diagram of Direct power control of DFIG

3.2 Concept of Direct Power Control (DPC):

The two basic notions used to determine the instantaneous switching state of the rotor side converter to control the active and reactive power are

- i) The stator active power can be controlled by controlling the angular position of the rotor flux vector.
- ii) The stator reactive power can be controlled by controlling the magnitude of the rotor flux vector [12].

Voltage vectors and their effects:

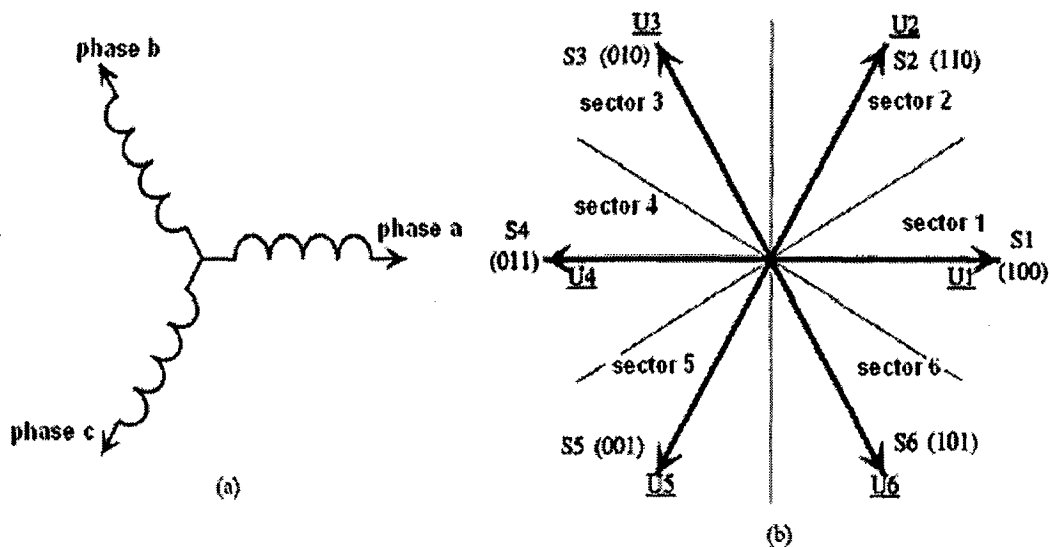


Fig. 3.2 (a) Orientation of the rotor winding in space with respect to which the voltage space phasors are drawn and (b) voltage space phasors [12].

Assuming that the orientation of the three phase rotor winding in space at any instant of time is as given in 3.2 (a), the six active switching states $S_1, S_2 \dots S_6$ would result in the voltage space vectors $U_1, U_2 \dots U_6$ at that instant as shown in Fig. 3.2 (b). In order to make an appropriate selection of the voltage vector the space phasor plane is first subdivided into six 60° sectors 1, 2...6. The instantaneous magnitude and angular velocity of the rotor flux can now be controlled by selecting a particular voltage vector depending on its present location. The effect of the different vectors

as reflected on the stator side active and reactive powers, when the rotor flux is positioned in Sector 1 is illustrated in the following subsections.

Considering anti clockwise direction of rotation of the flux vectors in the rotor reference frame to be positive, it may be noted that Ψ_s is behind Ψ_r in generating mode. This is illustrated in Fig. 3.3. In the rotor reference frame the flux vectors rotate in the positive direction at sub-synchronous speeds, remain stationary at synchronous speed and start rotating in the negative direction at super-synchronous speeds [12].

(A) Effect of Active Vectors on Active Power:

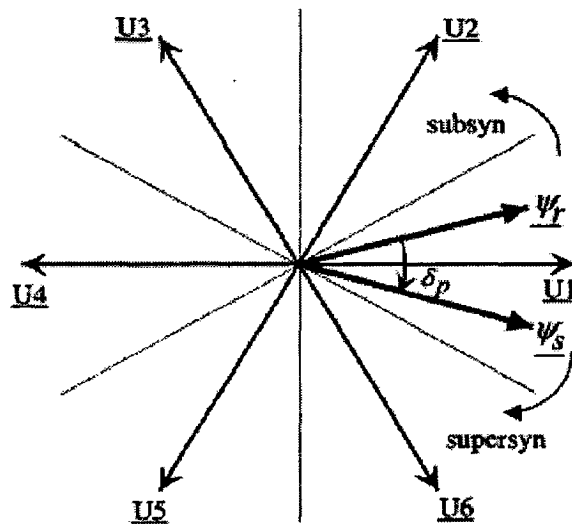


Fig 3.3: Flux vectors generating mode [12].

Assuming that the rotor flux is positioned in Sector 1, application of voltage vectors U_2 and U_3 accelerates Ψ_r in the positive direction results in an increase in angular separation between the two and thereby an increase in the active power generated by the stator. Similarly it can be seen that the effect of U_5 and U_6 on the active power would be exactly opposite to that of U_2 and U_3 .

It may therefore, be concluded that, if the rotor flux is in the K^{th} sector, where $K=1,2,3,\dots,6$ application of vectors $U(K+1)$ and $U(K+2)$ would result in increase in the stator active power generated and application of vectors $U(K-1)$ and $U(K-2)$ would result in reduction in the stator active power [12].

(B) Effect of Active Vectors on Reactive Power:

When the rotor flux vector is located in Sector 1, voltage vectors U_1 , U_2 and U_6 increase the magnitude of Ψ_r , whereas U_3 , U_4 and U_5 reduce it. An increase in magnitude of Ψ_r indicates an increased amount of reactive power being fed from the rotor side and hence, a reduction in the reactive power drawn by the stator resulting in an improved stator power factor. A decrease in magnitude of Ψ_r , amounts to lowering of the stator power factor.

As a generalization it can therefore, be said that if the rotor flux resides in the K^{th} sector, switching vectors $U(K)$, $U(K+1)$ and $U(K-1)$ reduce the reactive power drawn from the stator side and $U(K+2)$, $U(K-2)$ and $U(K+3)$ increase the reactive power drawn from the stator side [12].

C. Effect of Zero Vectors on Active Power:

The effect of the zero vectors is to stall the rotor flux without affecting its magnitude. This results in an opposite effect on the stator active power in sub-synchronous and super-synchronous modes of operation.

In sub-synchronous mode application of a zero vector decreases δ as Ψ_s keeps rotating in the positive direction at slip speed. Above the synchronous speed, Ψ_s rotates in the counter clockwise direction thereby increasing δ . Hence active power generated by the stator decreases for sub-synchronous operation and increases for super-synchronous operation [12].

(D) Effect of Zero Vectors on Reactive Power:

Since a zero vector does not change the magnitude of the rotor flux its effect on the reactive power is rather small. Nevertheless, there is some small change in Q_s ; its effect being dependent on whether the angle between the stator and rotor fluxes increases or decreases due to the application of a zero vector. An increase in angular separation between the two fluxes reduces Ψ_{rq} resulting in an increment of Q_s drawn from the stator side. The converse is true when δ reduces [12]. This is summarized in Table 3.1.

Table 3.1: Effect of Zero Vectors on Reactive Power [12]

Speed	Generating
Sub-synchronous	$\delta_p \downarrow \Rightarrow \Psi_{rq} \uparrow \Rightarrow Q_s \downarrow$
Super-synchronous	$\delta_p \uparrow \Rightarrow \Psi_{rq} \downarrow \Rightarrow Q_s \uparrow$

Note: \uparrow denotes increase and \downarrow denotes decrease

3.3 Implementation of Direct power control algorithm in Simulink:

The reference for the stator active power can be calculated as $P_s^* = T_{ref} * \omega_s$ and Q_s^* is selected depends on the requirement of power factor. The active and reactive powers on the stator side can be directly computed from the stator currents and voltages.

DPC algorithm:

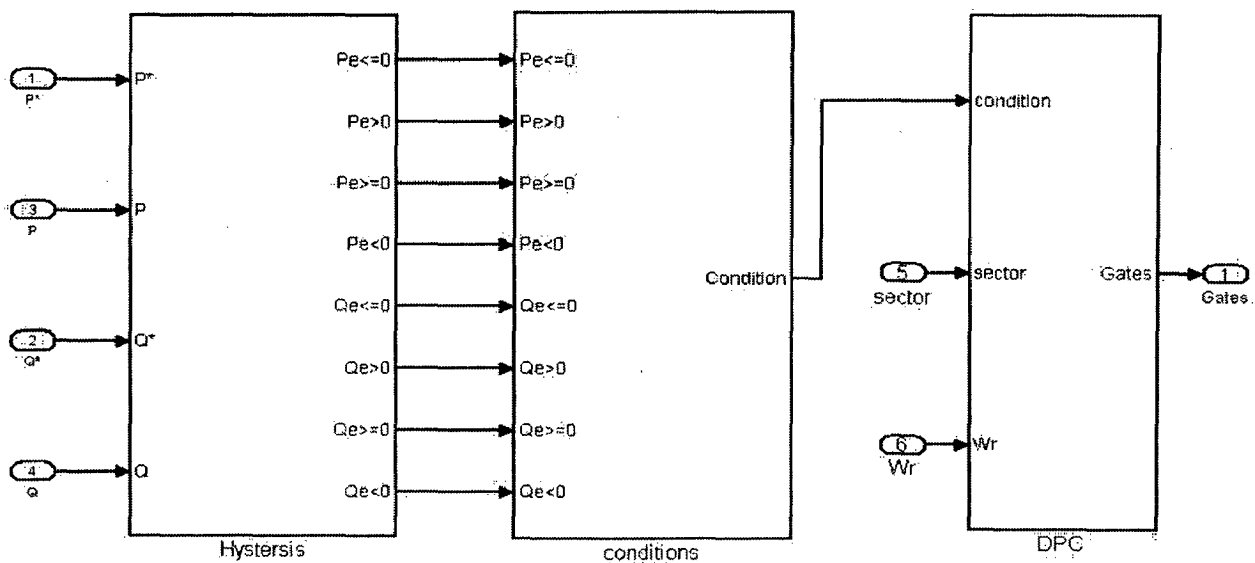


Fig 3.4: Simulink model of direct power control scheme

Hysteresis controllers:

P_s^* is the reference for stator active power. The actual active power P_s is to be controlled to stay within a band of width P_{band} about P_s^* .

Similarly Q_s^* is the reference for stator reactive power. The actual reactive power Q_s is to be controlled to stay within a band of width Q_{band} about Q_s^* . This is modeled as shown in fig 3.5

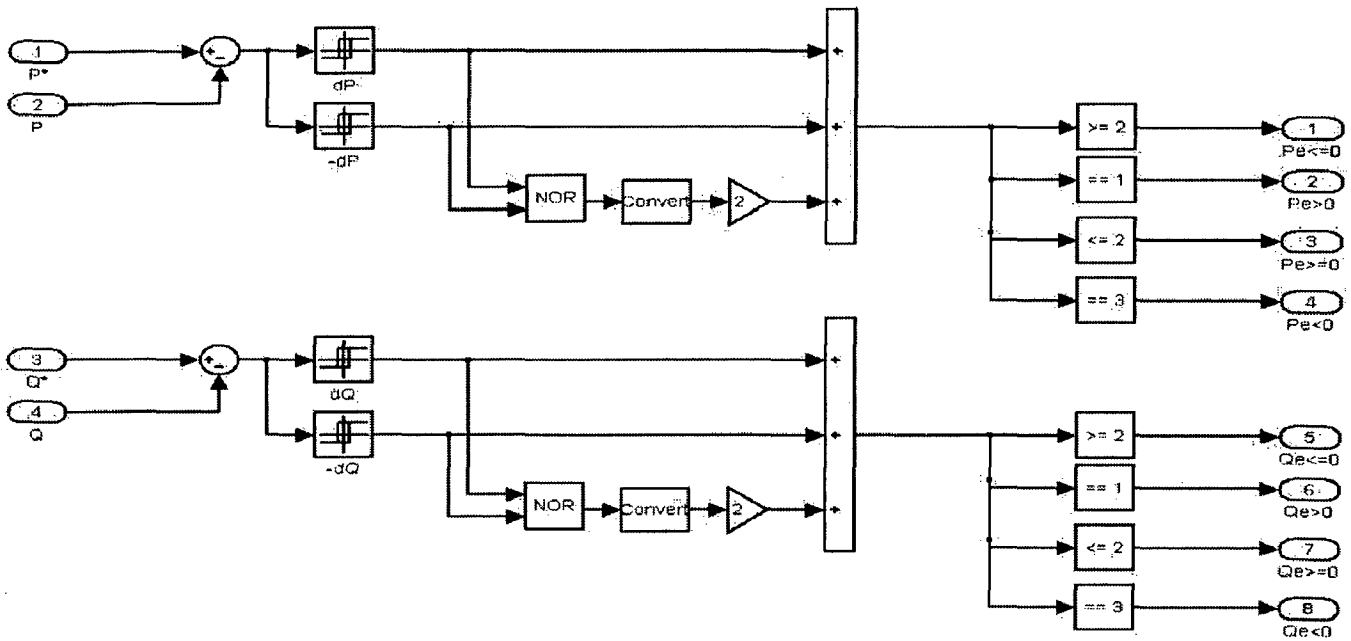


Fig 3.5: Simulink model of Hysteresis controllers

Conditions according to power requirements:

In order to determine the appropriate switching vector at any instant of time, the errors in P_s and Q_s , and the sector in which the rotor flux vector is presently residing are taken into consideration. Thus the following two switching tables for active vector selection can be generated. Tables 3.2 and 3.3 [12] correspond to negative and positive, active power errors respectively. If the rotor side converter is switched in accordance to these tables it is possible to control the active and reactive powers in the stator side within the desired error bands.

Table 3.2: Selection of Active switching states when ($P_{err} \leq 0$)

	Sector1	Sector 2	Sector 3	Sector 4	Sector 5	Sector 6
$Q_{err} > 0$	S3	S4	S5	S6	S1	S2
$Q_{err} \leq 0$	S2	S3	S4	S5	S6	S1

Table 3.3: Selection of Active switching states when ($P_{err} > 0$)

	Sector 1	Sector 2	Sector 3	Sector 4	Sector 5	Sector 6
$Q_{err} > 0$	S5	S6	S1	S2	S3	S4
$Q_{err} \leq 0$	S6	S1	S2	S3	S4	S5

By considering the effect of the zero vector on active and reactive powers, the logic for selecting the zero vector can be summarized as in Table 3.4 [12]. Whenever a zero vector has to be applied, the one nearest to the present active vector is selected to minimize the number of switchings.

Table 3.4: Condition for selection of zero vectors

Speed	
Sub-Synchronous speed	$Q_{err} < 0$ And $P_{err} >= 0$
Super-Synchronous speed	$P_{err} < 0$ And $Q_{err} \leq 0$

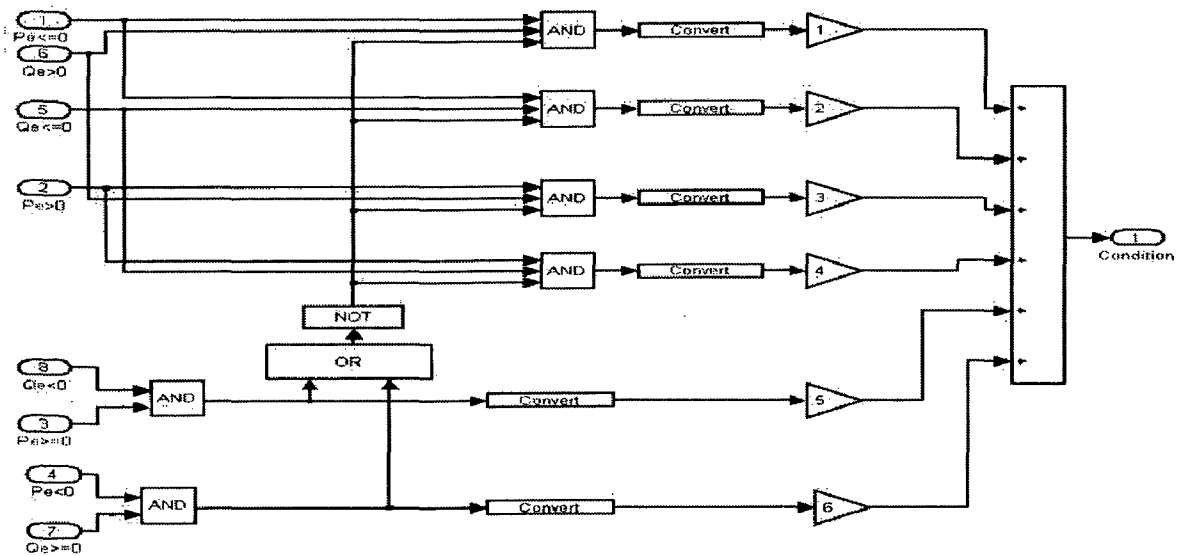


Fig 3.6: Simulink model for producing conditions

Pulse Generation:

With the inferences drawn in the previous section it is possible to switch an appropriate voltage vector in the rotor side at any given instant of time to increase or decrease the active or reactive power in the stator side. Therefore, any given references for stator active and reactive powers can be tracked within a narrow band by selecting proper switching vectors for the rotor side converter.

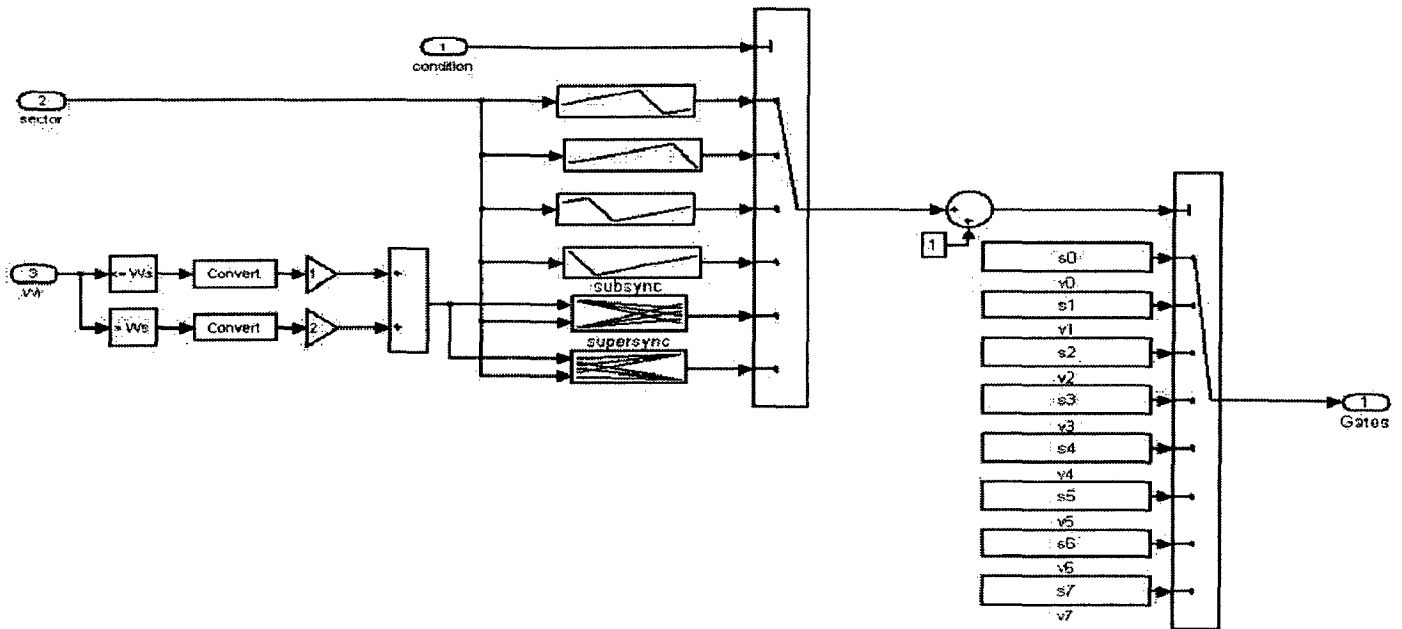


Fig 3.7: Simulink model of Pulse generation

Sector Identification:

This method uses integration of the PWM rotor voltage to compute the rotor flux. Then the flux angle is calculated hence the sector in which the rotor flux resides can be identified.

$$\begin{aligned}
 F_{rd} &= \int (V_{rd} - R_r I_{rd}) dt \\
 F_{rq} &= \int (V_{rq} - R_r I_{rq}) dt \\
 \theta_r &= \tan^{-1} \frac{F_{rq}}{F_{rd}}
 \end{aligned}
 \tag{3.1}$$

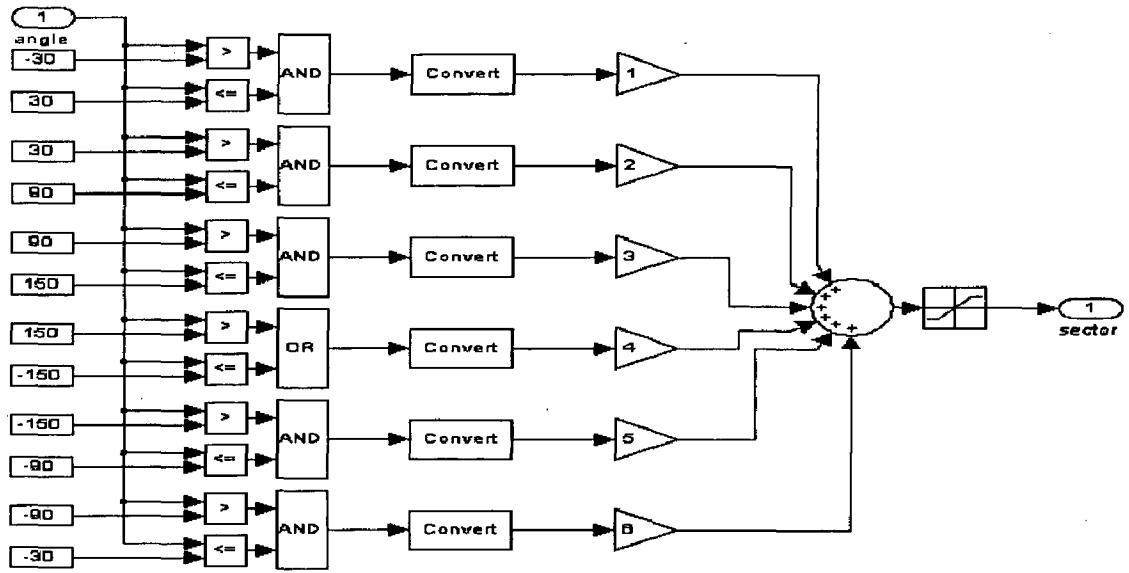


Fig 3.8: Simulink model of sector identification

Complete system modeling in simulink:

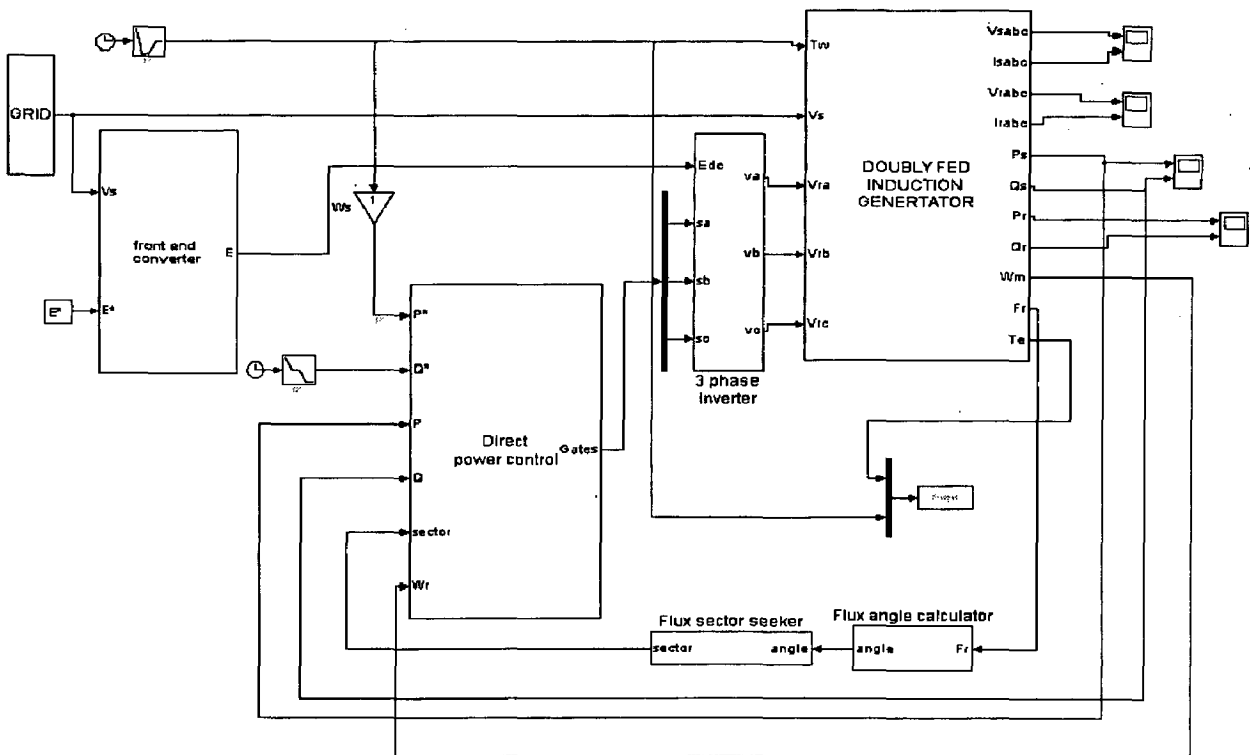


Fig 3.9: Modeling of the direct power control of DFIG system in simulink

3.4 Simulation Results:

The direct power control algorithm is simulated on the MATLAB-SIMULINK platform. The transient response due to a step change in active and reactive power commands is shown in Fig. 3.10 and 3.11. P_{band} and Q_{band} are kept at 0.05 p.u. in this case.

It is observed that P_s reaches its set value in approximately 1ms. And Q_s reaches its set value in approximately 15ms this can be the fastest possible response because only the desired active vector is used during the transient.

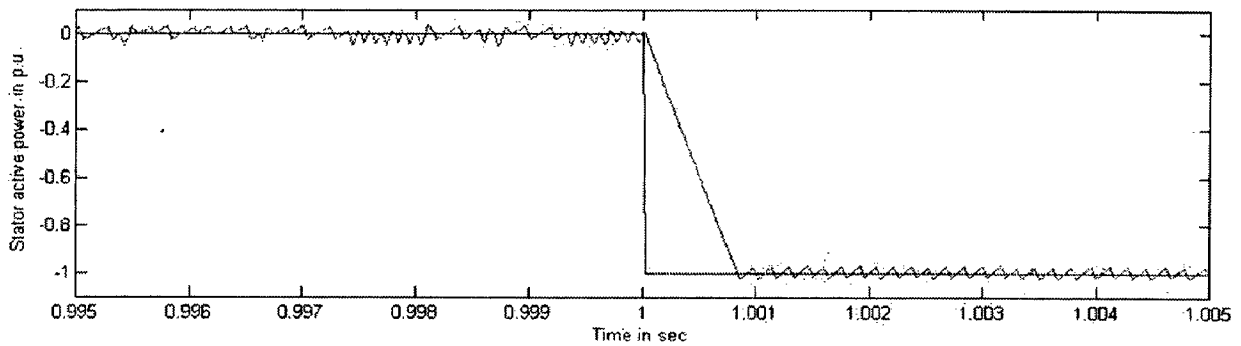


Fig 3.10: Response of stator active power for step change in reference active power

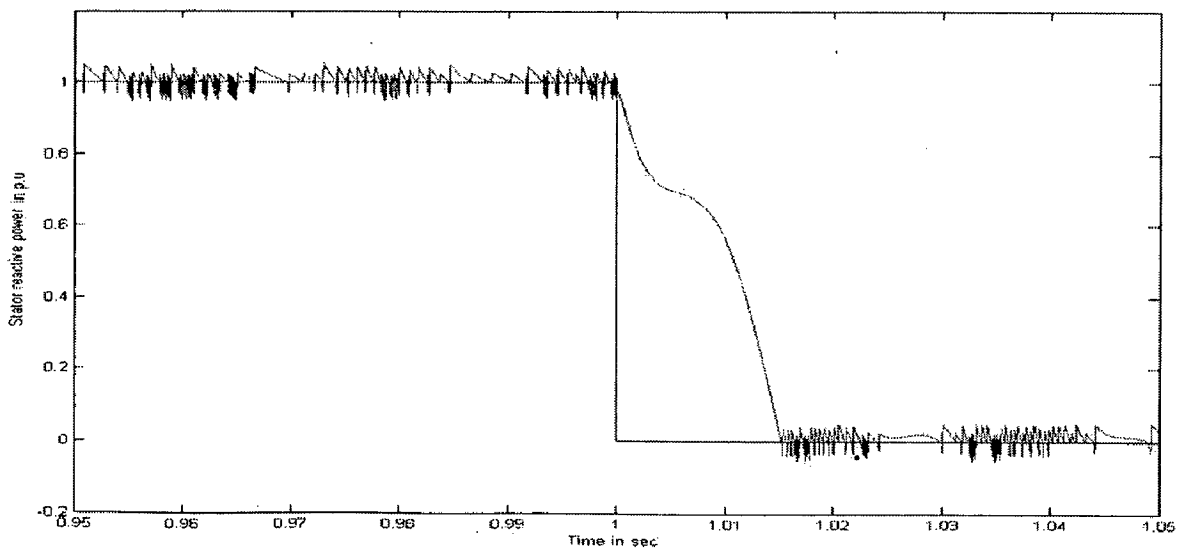


Fig 3.11: Response of reactive power for step change in reference reactive power

Response of P_s for different values of P_s^* :

In the figure stator reference active power and actual stator active power are shown. P_s follows P_s^* with in certain hysteresis band of band width P_{band} . Stator active power is taken as negative as it feeds active power to the grid.

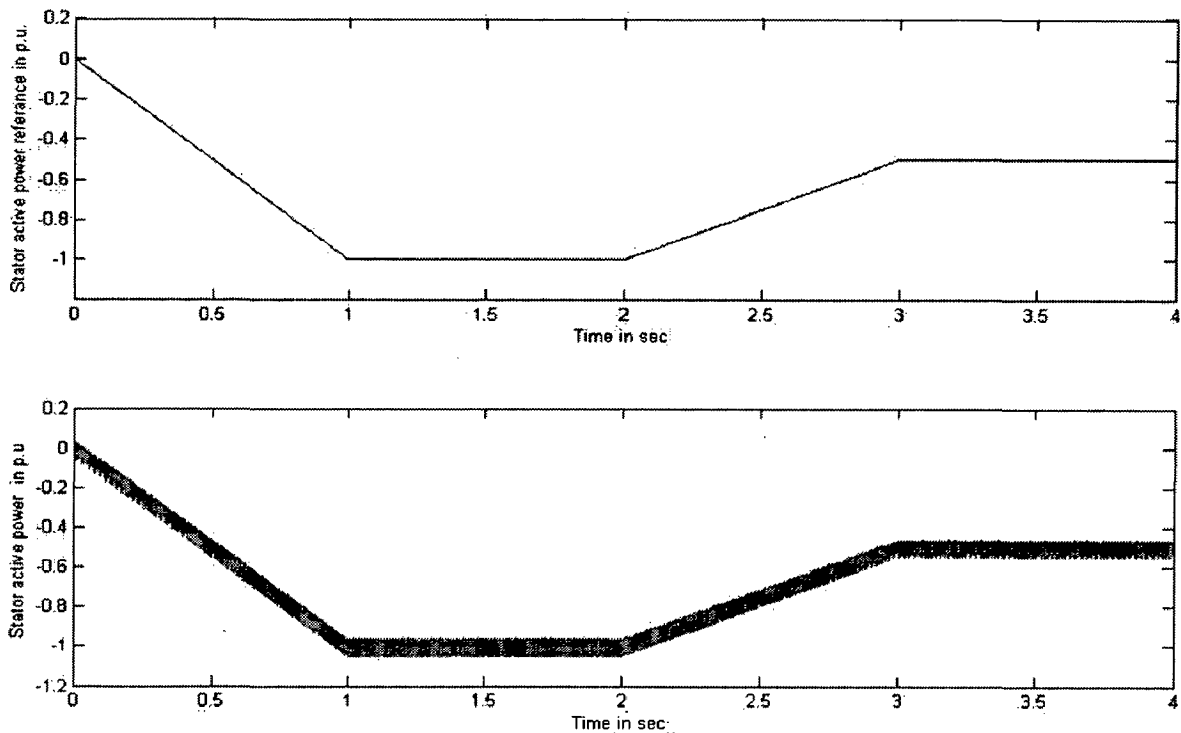


Fig 3.12: Response of P_s for different values of P_s^*

The dynamic response of the system is very good as the rise time is in mille seconds. So this type of control technique will be suitable in optimum power tracking for maximum energy capture in a wind energy application. The optimum power varies with the speed of the turbine and by using this control the stator power is maintained at equal to the optimum power.

Response of Q_s for different values of Q_s^* :

In the figure stator reference reactive power and actual stator reactive power are shown. Q_s Follows Q_s^* with in certain hysteresis band of band width Q_{band} . Stator reactive power is taken as positive as it takes reactive power from the grid.

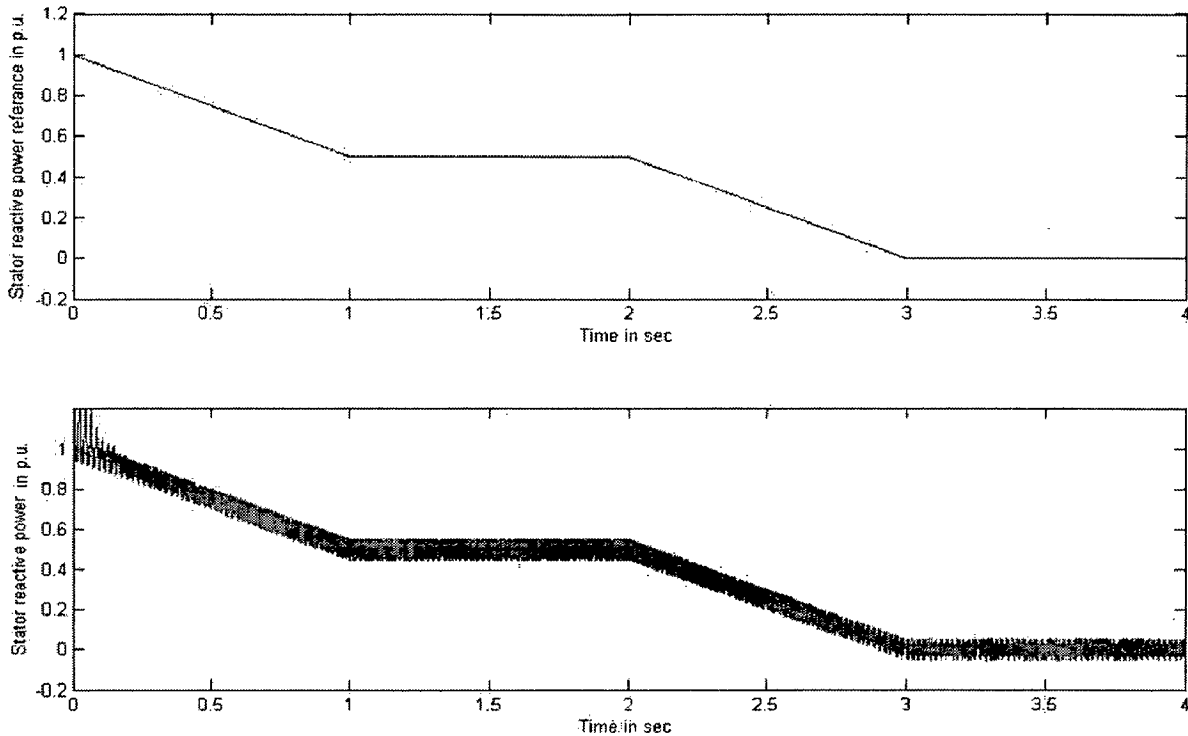


Fig 3.13: Response of Q_s for different values of Q_s^*

So we can control the stator reactive power as per our requirement, so that we can control the power factor of the system. Hence the overall system power factor can be kept at unity under varying conditions of load.

This system has excellent dynamic response and decoupled control of active and reactive powers as shown by the simulation results. Since it depends only on voltage and current measurements on the stator side, it is insensitive to the parameters of the machine.

Response of Stator current for different values of P_s and Q_s :

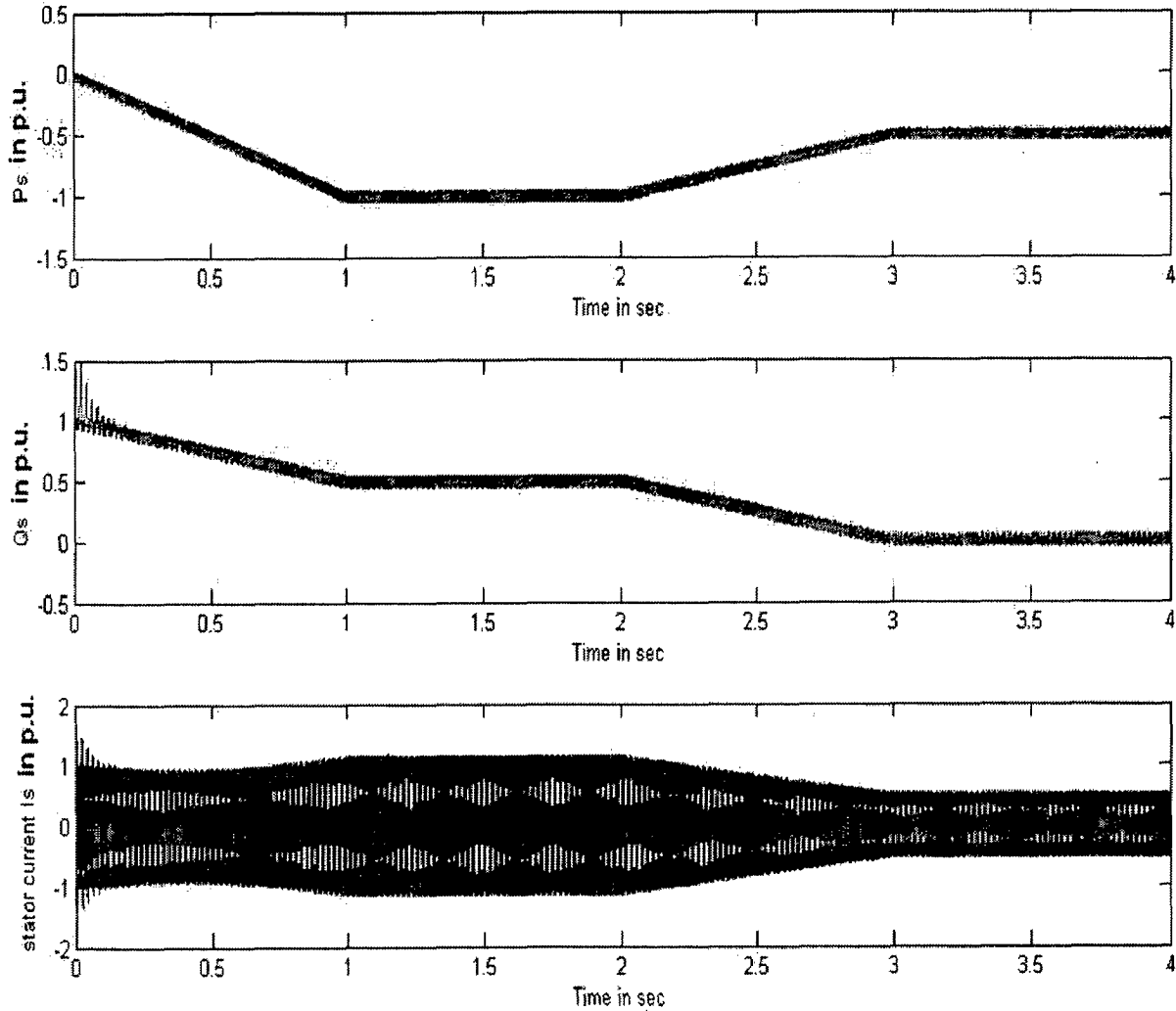


Fig 3.14: Response of Stator current for different values of P_s and Q_s

The variation in stator current with change in active and reactive powers is shown in the fig 3.14. In the figure, from 0 to 1sec active power generation is increasing and reactive power drawn is reducing and as current is proportional to the KVA the change in current is very less. From 1 to 2 sec P_s and Q_s are constant hence current is constant. From 2 to 3 sec both P_s and Q_s are reducing hence current is reduced.

Stator voltage and current:

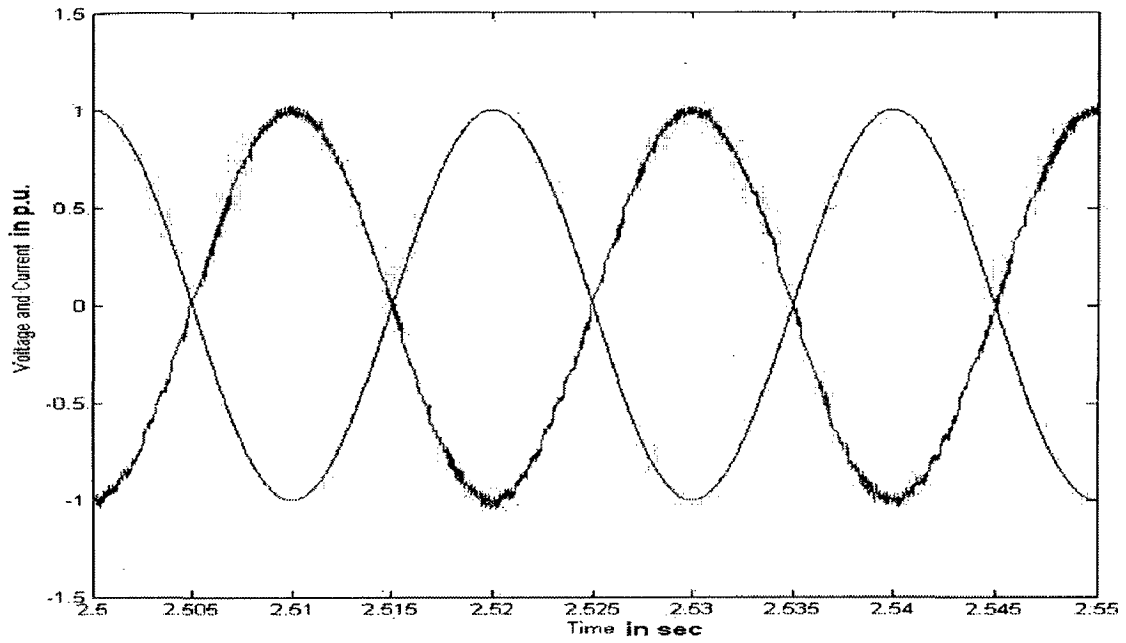


Fig 3.15: V_s and I_s when $Q_s = 0$ p.u.

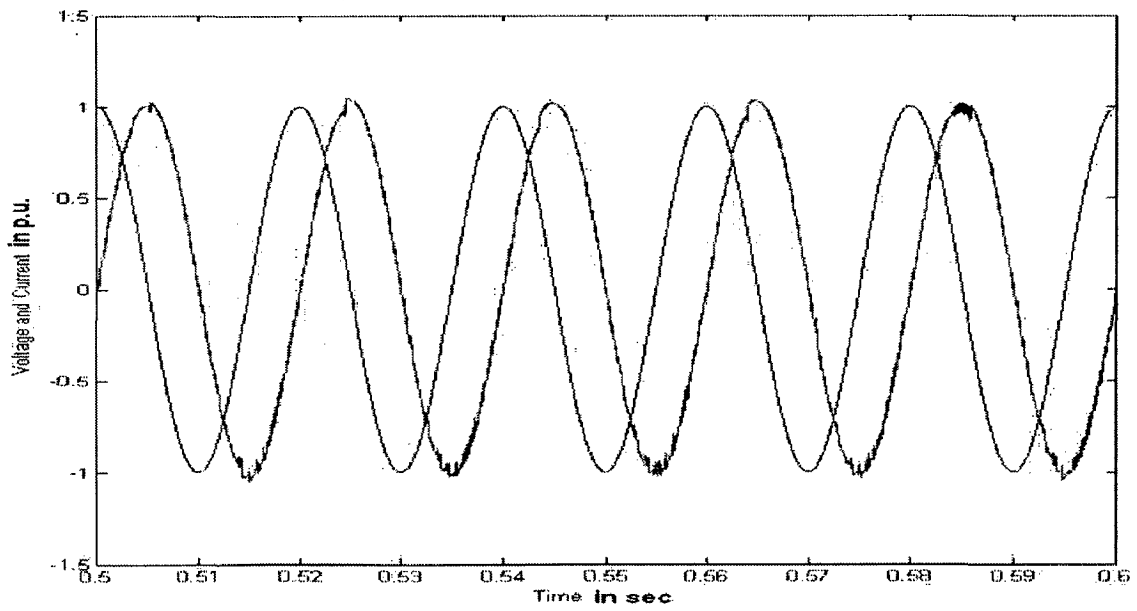


Fig 3.16: V_s and I_s when $Q_s = 1$ p.u. and $P_s = 0$ p.u.

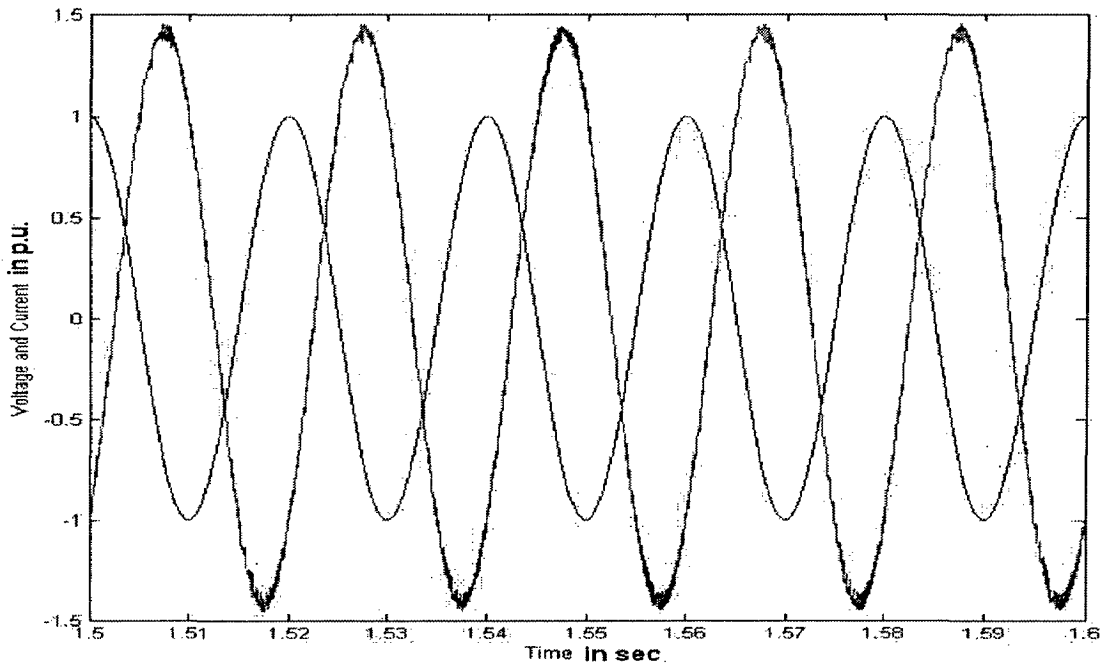


Fig 3.17: V_s and I_s when $Q_s=1$ p.u. and $P_s=1$ p.u.

When reactive power drawn by stator is zero that means the KVA is only active power then the current lags the voltage by angle of 180° . So the power factor is unity and stator power is negative. When the reactive power drawn is one p.u and active power drawn is zero hence the KVA is only reactive power then the current lags the voltage by 90° hence the power factor is zero. So that we can control the stator power factor from zero to unity.

Response of active power with d-axis component of current:

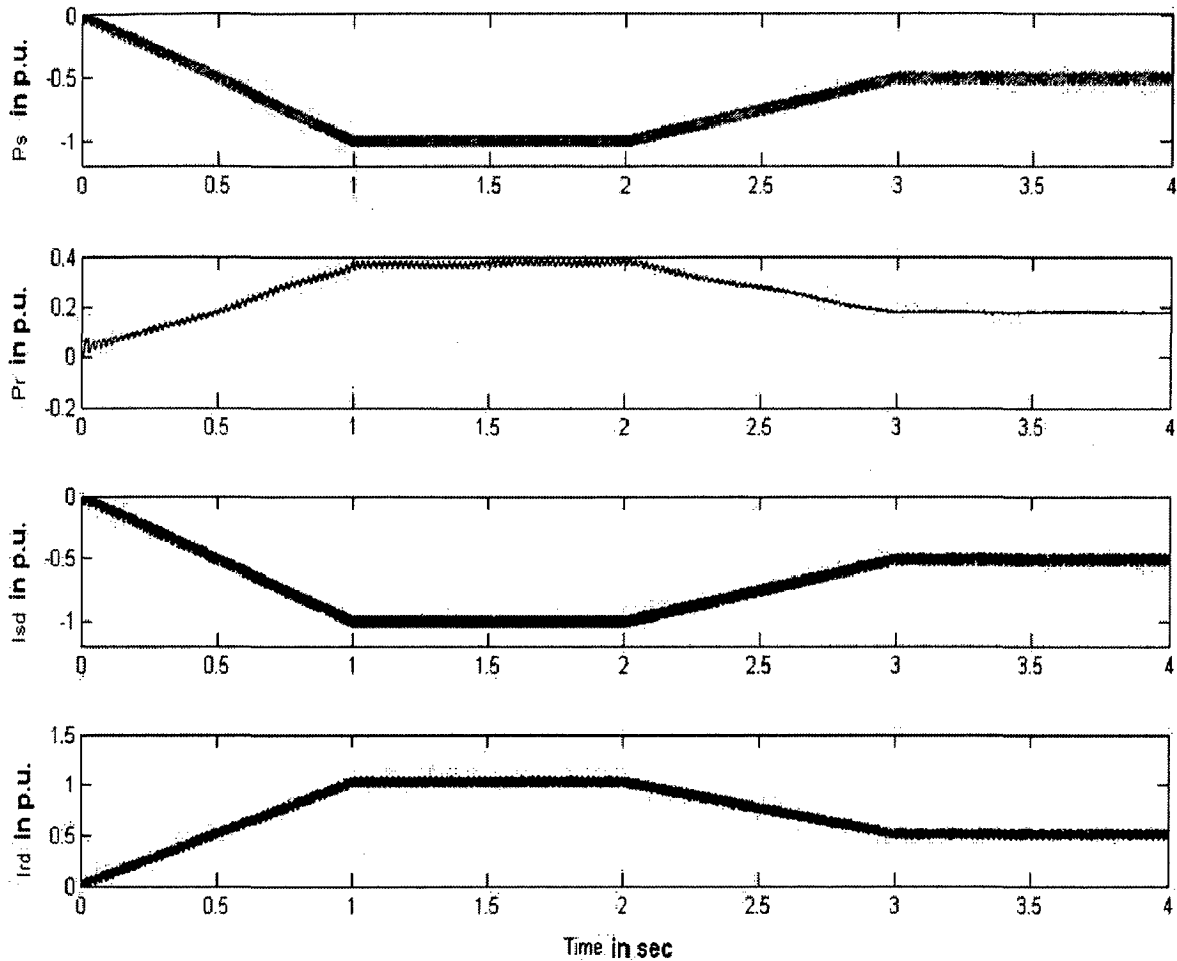


Fig 3.18: Response of active power with d-axis component of current

P_s is controlled by controlling d-axis component of stator current (I_{sd}). And similarly P_r is controlled by controlling I_{rd} . And $I_{sd} = -I_{rd}$ always. So by controlling I_{rd} we can control stator active power. So with the change in the reference active power the d-axis current injected from rotor side changes then as I_{sd} is proportional to I_{rd} , I_{sd} changes which in turn result in the variation in actual stator active power.

Response of reactive power with q-axis component of current:

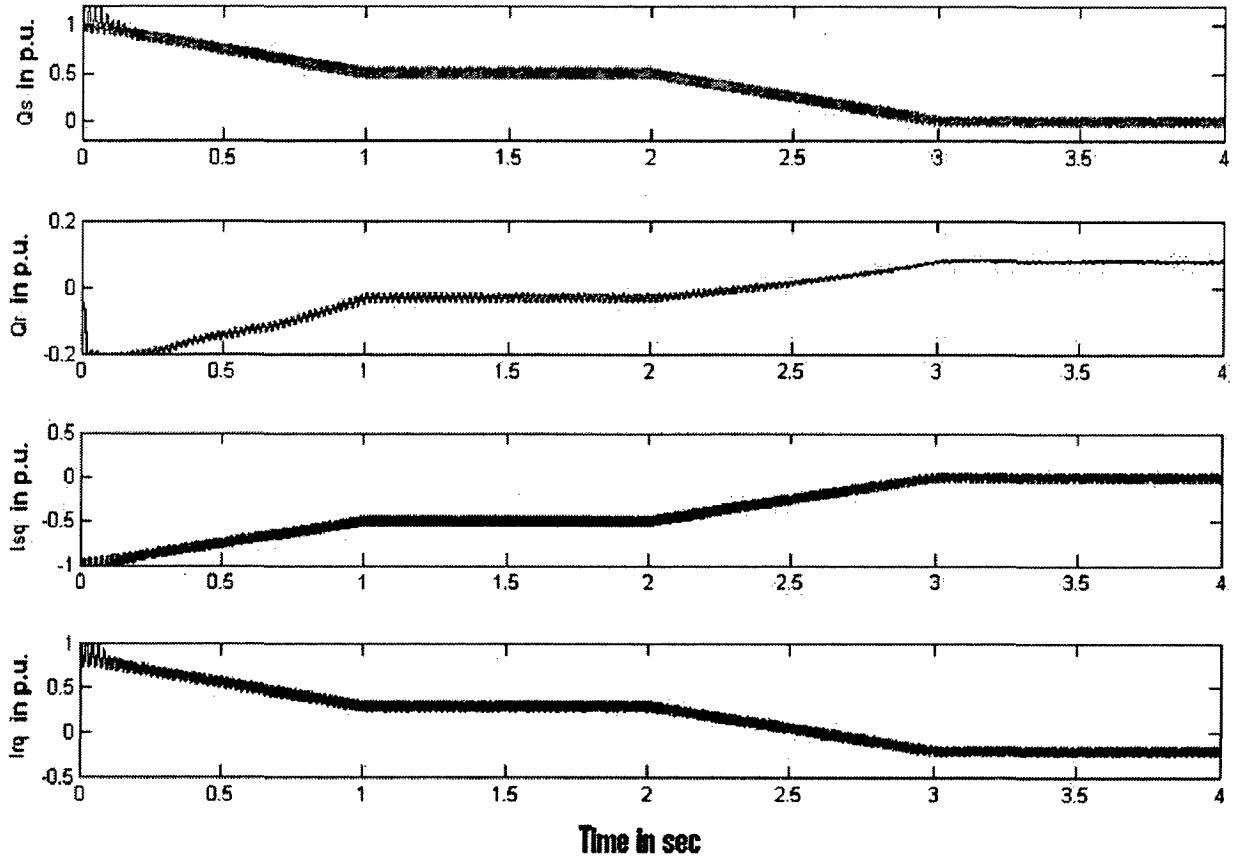


Fig 3.19: Response of reactive power with q-axis component of current

Q_s is controlled by controlling I_{sq} and Q_r is controlled by controlling I_{rq} . And $I_{sq} + I_{rq} = I_{ms}$ (magnetizing current). And I_{ms} is always constant. So depends on the reference reactive power if we inject I_{rq} from rotor side I_{sq} drawn will be less hence the reactive power drawn from the stator is controlled hence stator power factor can be controlled.

3.5 Comparison of DPC with vector control:

The Figure 3.20 given below shows the model of vector control of DFIG. In this rotor side control is controlled by using vector control. The stator active and reactive powers are tracked by using PI controllers and depending upon the error in active and reactive powers I_{rd} and I_{rq} is injected to the rotor by applying V_{rd} and V_{rq} . By these reference values of V_{rd} and V_{rq} we have to give pulses to the rotor side inverter.

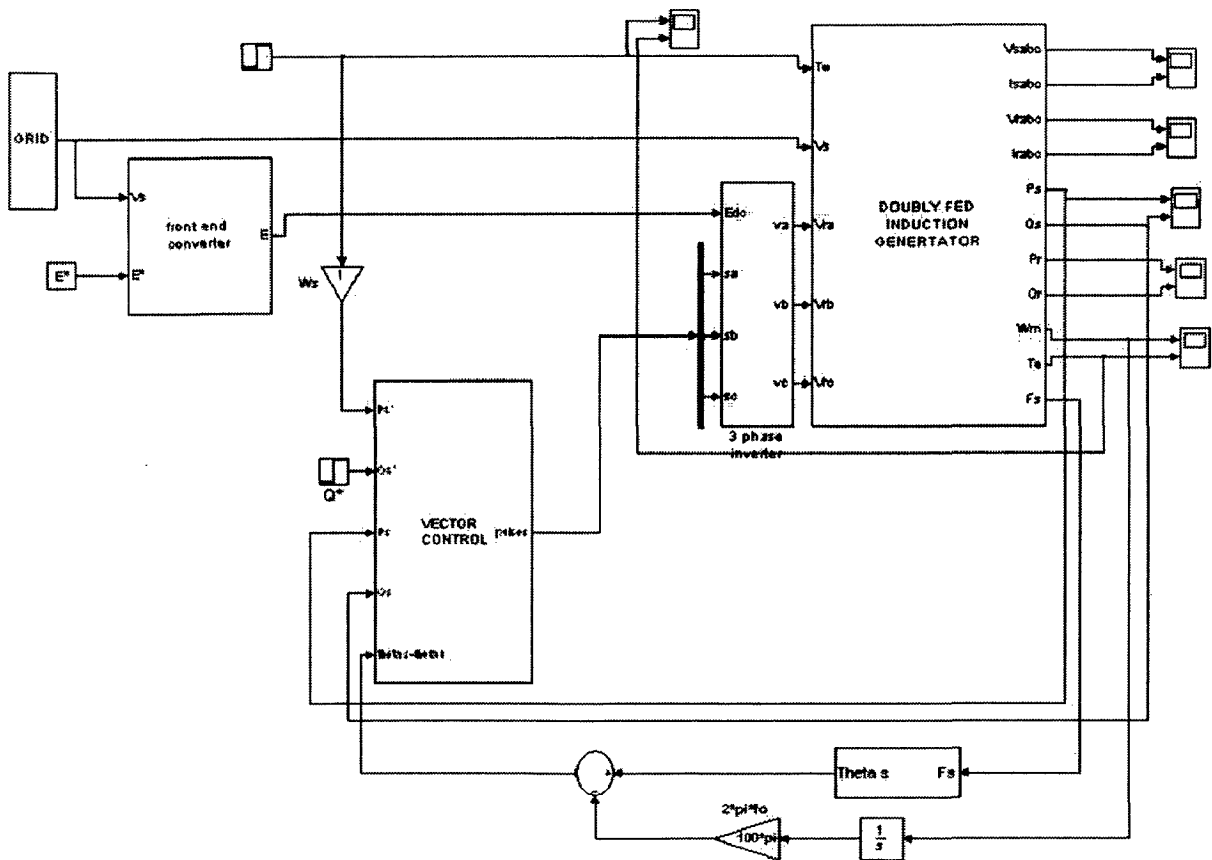


Fig 3.20: modeling of vector control of DFIG

This method uses the integration of the Stator voltage to compute the stator flux then the stator angle can be calculated.

Active and reactive powers for a step change in reference values:

The independent control of stator active and reactive power can be obtained by this vector control scheme as shown by the simulation results. Response of reference active and reactive powers is shown below for the step change in reference active and reactive powers.

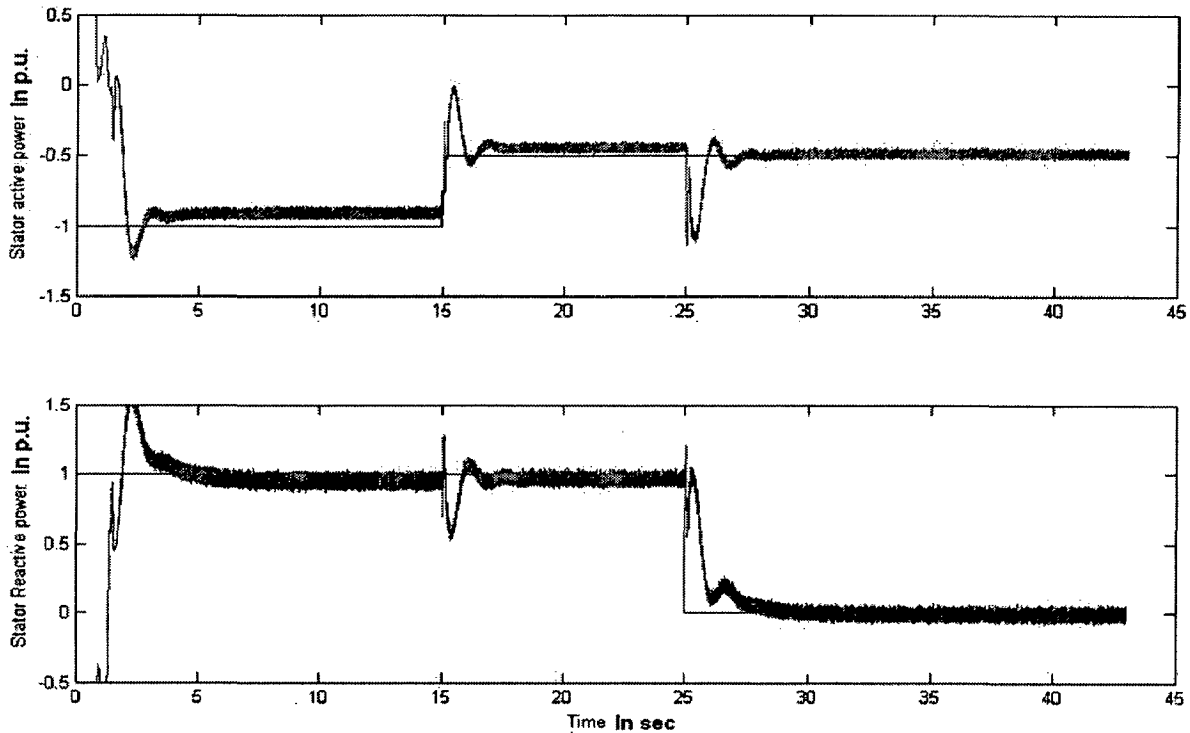


Fig 3.23 Response of active and reactive power for a step change in reference powers

The system performance depends on the accuracy of calculation of flux angle and the accuracy of position encoder. The dynamic response of the system is very slow compared with DPC as the settling time in the case of vector control is in the range of 2 to 3 secs where as in case of DPC it is in mille seconds. The peak overshoot in case of vector control is high where as in case of DPC the actual values vary with in the band. The steady state error is approximately same in both the cases.

3.5 Comparison of DPC with vector control:

The Figure 3.20 given below shows the model of vector control of DFIG. In this rotor side control is controlled by using vector control. The stator active and reactive powers are tracked by using PI controllers and depending upon the error in active and reactive powers I_{rd} and I_{rq} is injected to the rotor by applying V_{rd} and V_{rq} . By these reference values of V_{rd} and V_{rq} we have to give pulses to the rotor side inverter.

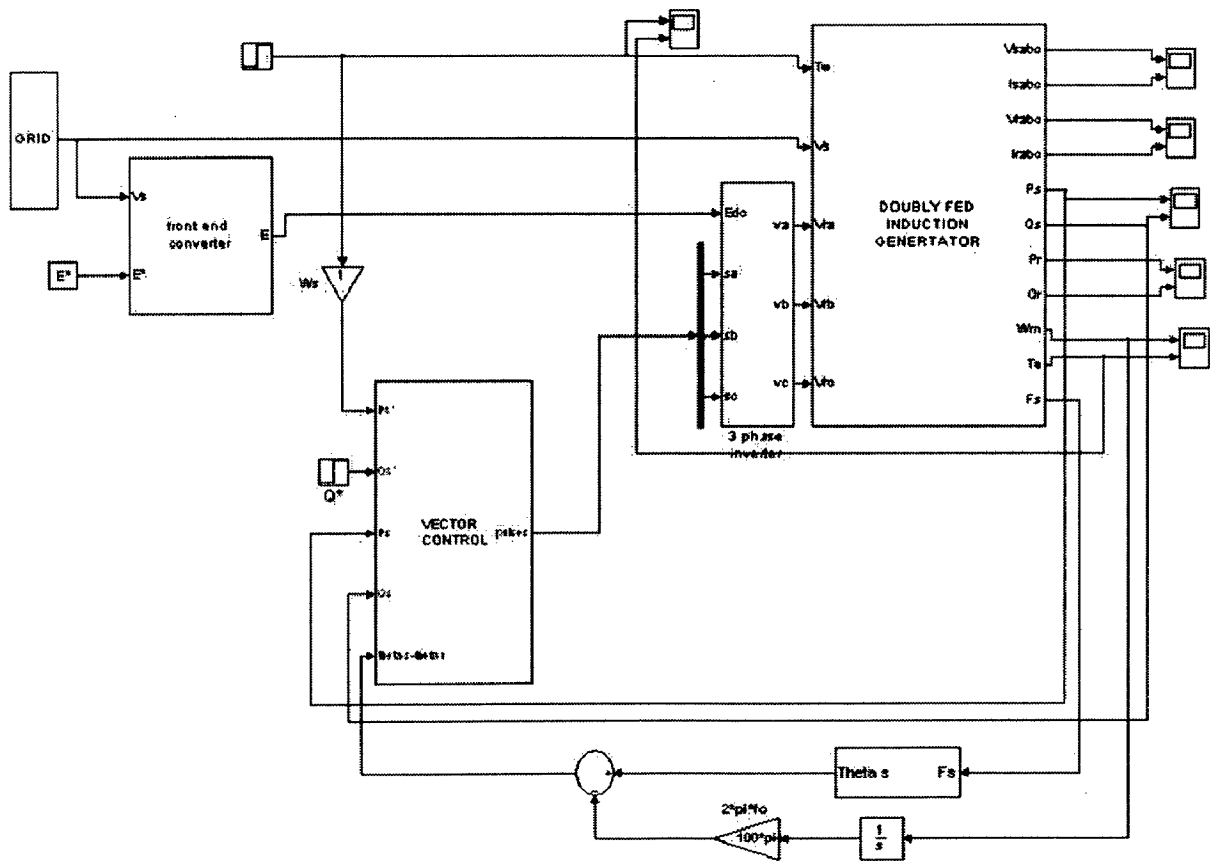


Fig 3.20: modeling of vector control of DFIG

This method uses the integration of the Stator voltage to compute the stator flux then the stator angle can be calculated.

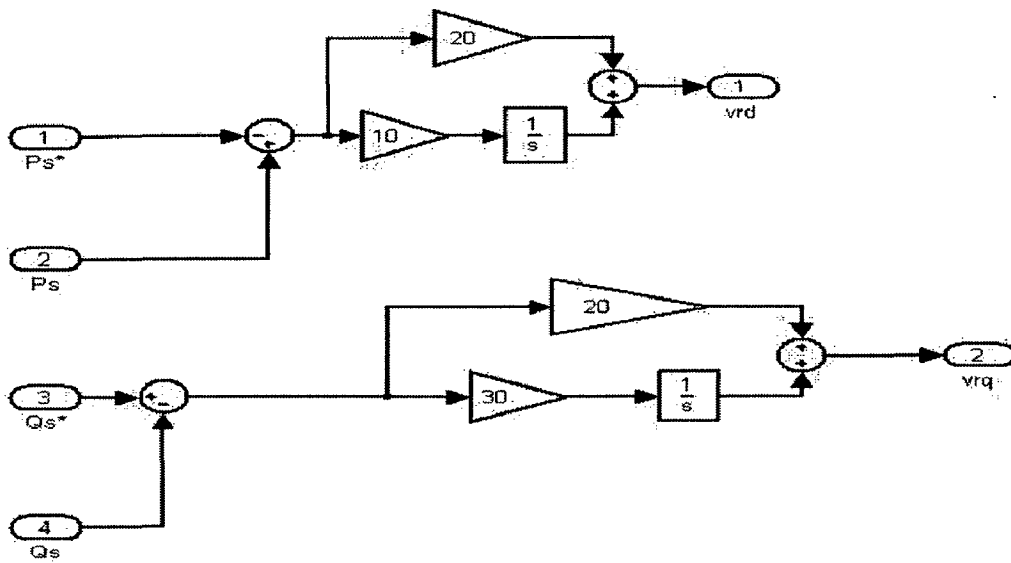


Fig 3.21: PI controllers used in tracking of active and reactive powers

Here the active power can be controlled by injecting d-axis component of rotor current. As I_{rd} can be controlled by controlling V_{rd} . Hence stator active power can be controlled by V_{rd} . Similarly stator reactive power can be controlled by varying V_{rq} . The rotor angle is calculated by sensing the rotor speed for converting the reference rotor voltages of rotating dq frame into abc frame.

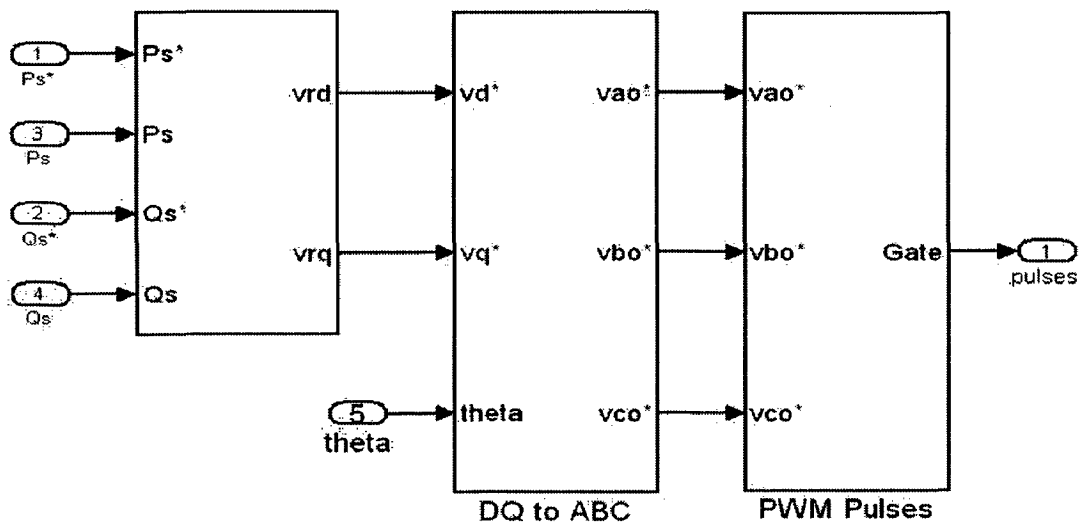


Fig 3.22 Vector control scheme for machine side converter

Active and reactive powers for a step change in reference values:

The independent control of stator active and reactive power can be obtained by this vector control scheme as shown by the simulation results. Response of reference active and reactive powers is shown below for the step change in reference active and reactive powers.

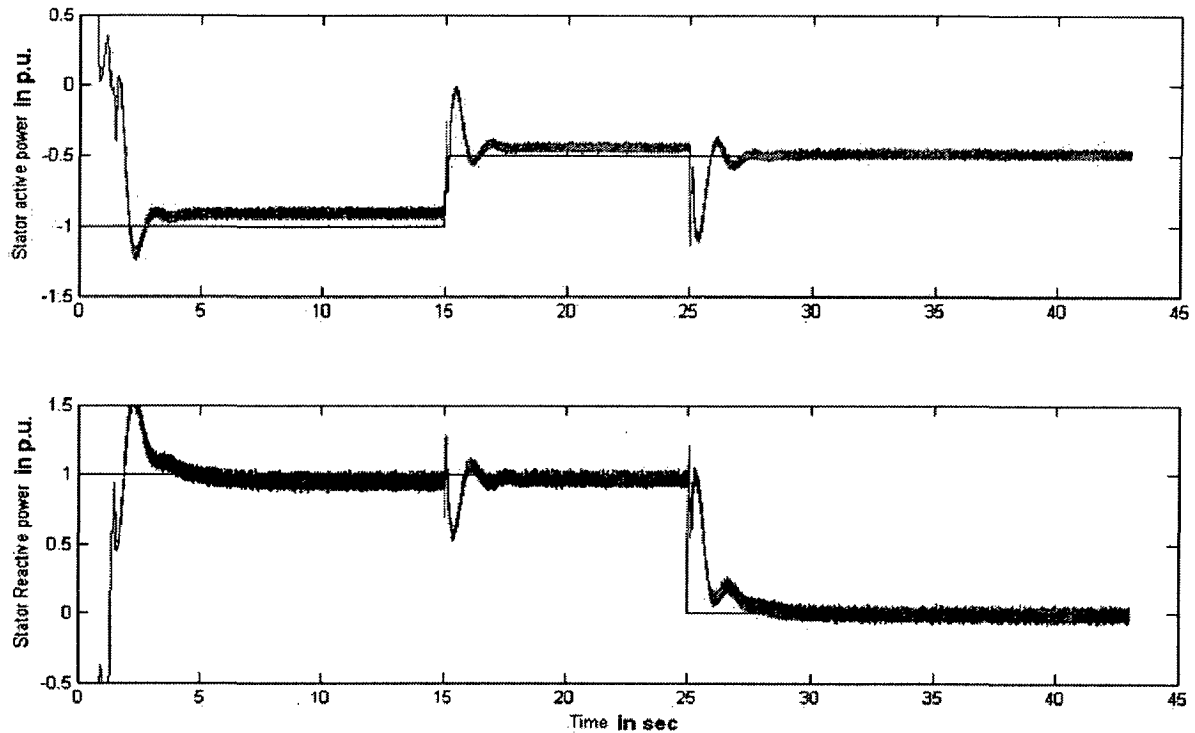


Fig 3.23 Response of active and reactive power for a step change in reference powers

The system performance depends on the accuracy of calculation of flux angle and the accuracy of position encoder. The dynamic response of the system is very slow compared with DPC as the settling time in the case of vector control is in the range of 2 to 3 secs where as in case of DPC it is in mille seconds. The peak overshoot in case of vector control is high where as in case of DPC the actual values vary with in the band. The steady state error is approximately same in both the cases.

Wind Turbine

4.1 Introduction:

In recent years there has been an increased attention toward wind power generation. Wind power has proven to be a potential source for generation of electricity with minimal environmental impact. With the advancement of aerodynamic designs, wind turbines that can capture several megawatts of power are available. When such wind energy conversion systems are integrated to the grid, they produce a substantial amount of power which can supplement the base power generated by thermal, nuclear, or hydro power plants [14].

4.2 Wind Turbine modeling:

The wind turbine with optimum power control and pitch angle control is modeled in simulink. As shown in fig 4.1 the external inputs to the turbine are wind speed and rotor speed. Optimum power P_{opt} is obtained from the power-speed characteristics and it depends on the speed of the turbine.

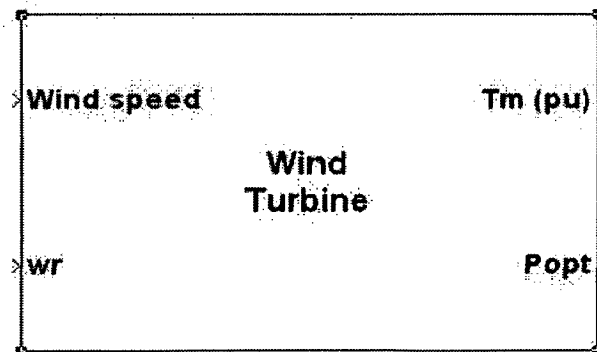


Fig 4.1: Simulink model of wind turbine with optimum power control

The model of wind turbine is based on the steady-state power characteristics of the turbine. The stiffness of the drive train is infinite and the friction factor and the inertia of the turbine must be combined with those of the generator coupled to the turbine.

The output power of the turbine is given by the following equation.

$$P_m = C_p (\lambda, \beta) \frac{\rho A}{2} (v_{wind})^3 \dots\dots\dots (4.1)$$

Where

P_m Mechanical output power of the turbine (W)

C_p Performance coefficient of the turbine

ρ Air density (kg/m³)

A Turbine swept area (m²)

V_{wind} Wind speed (m/s)

λ Tip speed ratio of the rotor blade tip speed to wind speed

β Blade pitch angle (deg)

Equation 4.1 can be normalized. In the per unit (pu) system we have:

$$P_{m_pu} = K_p C_{p_pu} v_{wind_pu}^3 \dots\dots\dots (4.2)$$

Where

P_{m_pu} Power in pu of nominal power for particular values of ρ and A

C_{p_pu} Performance coefficient in pu of the maximum value of c_p

V_{wind_pu} Wind speed in pu of the base wind speed.

K_p Power gain for C_{p_pu}=1 pu and V_{wind_pu}=1 pu, k_p is less than or equal to 1

A generic equation is used to model $C_p(\lambda, \beta)$ is

$$C_p(\lambda, \beta) = C_1 \left(\frac{C_2}{\lambda_i} - C_3 \beta - C_4 \right) e^{\frac{-C_5}{\lambda_i}} + C_6 \lambda \quad \dots \dots \dots (4.3)$$

With

$$\frac{1}{\lambda_i} = \frac{1}{\lambda + 0.08 \beta} - \frac{0.035}{\beta^3 + 1} \quad \dots \dots \dots (4.4)$$

Where $C_1 = 0.5176$, $C_2 = 116$, $C_3 = 0.4$, $C_4 = 5$, $C_5 = 21$ and $C_6 = 0.0068$.

The C_p - λ characteristics, for different values of the pitch angle β , are illustrated below on fig 4.2. The maximum value of C_p ($C_{pmax} = 0.48$) is achieved for $\beta = 0$ degree and for $\lambda = 8.1$. This particular value of λ is defined as the nominal value (λ_{nom}).

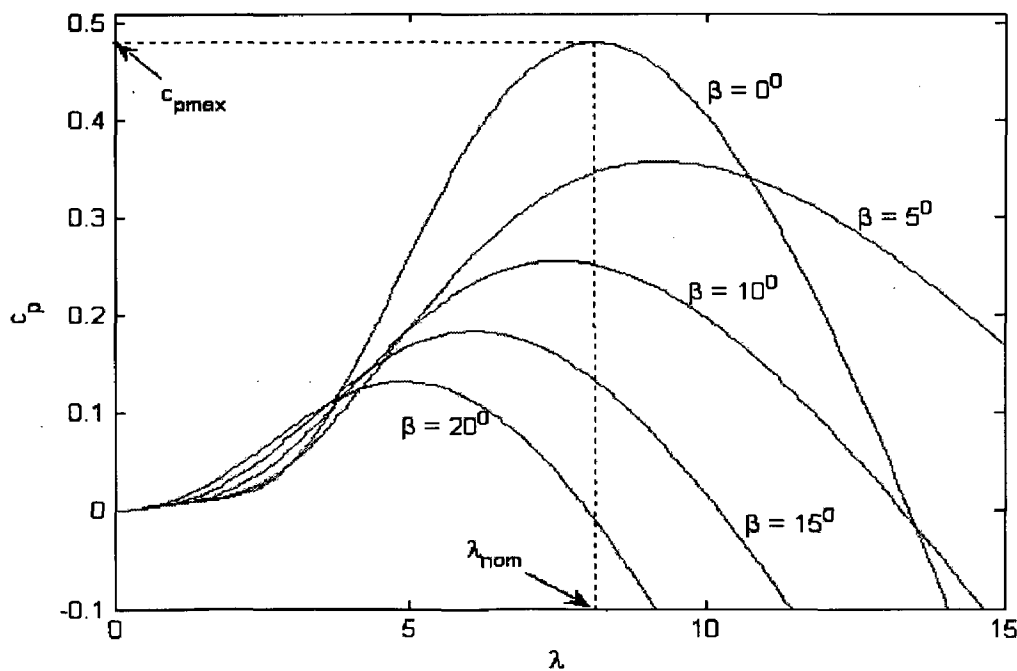


Fig 4.2: C_p - λ characteristics

The Simulink model of the turbine is illustrated in the following figure. The three inputs are the generator speed (ω_{r_pu}) in pu of the nominal speed of the generator, the pitch angle in degrees and the wind speed in m/s. The tip speed ratio λ in pu of λ_{nom} is obtained by the division of the rotational speed in pu of the base rotational speed and the wind speed in pu of the base wind speed. The output is the torque and is applied to the generator shaft.

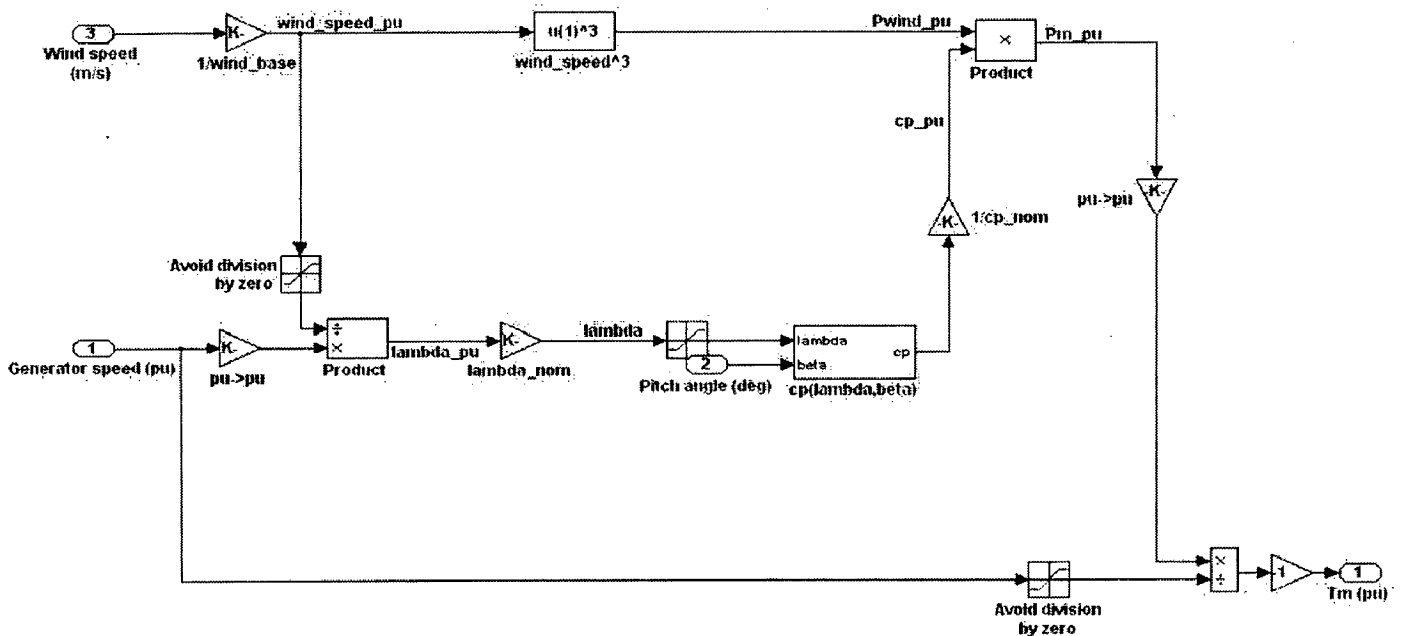


Fig 4.3 Simulink model of the wind turbine

Output of the mechanical torque of the wind turbine, in pu of the nominal generator torque. The nominal torque of the generator is based on the nominal generator power and speed.

4.3 Optimum power control:

The power is controlled in order to follow a pre-defined power-speed characteristic, named tracking characteristic. Such a characteristic is illustrated by the ABCD curve superimposed on the mechanical power characteristics of the turbine obtained at different wind speeds. The actual speed of the turbine ω_r is

measured and the corresponding mechanical power of the tracking characteristic is used as the reference power for the power control loop.

The tracking characteristic is defined by four points: A, B, C and D. From zero speed to speed of point A the reference power is zero. Between point A and point B the tracking characteristic is a straight line, the speed of point B must be greater than the speed of point A. Between point B and point C the tracking characteristic is the locus of the maximum power of the turbine. The tracking characteristic is a straight line from point C to point D. The power at point D is one per unit (1 pu) and the speed of the point D must be greater than the speed of point C. Beyond point D the reference power is a constant equal to one per unit (1 pu).

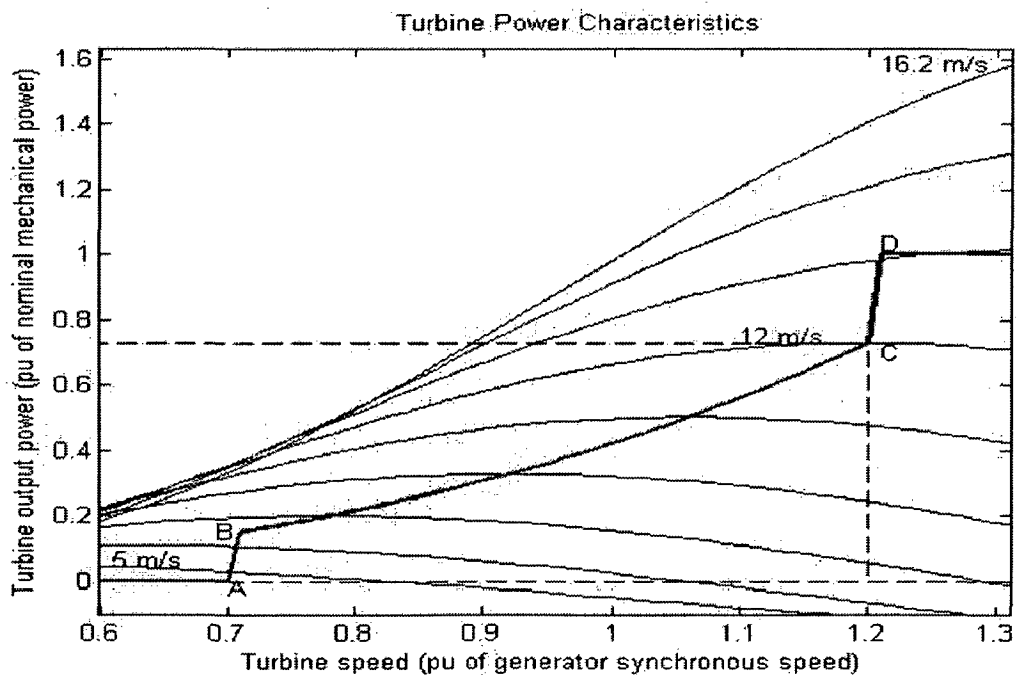


Fig 4.4 Turbine power characteristics and Tracking characteristics

In the fig 4.4 curve ABCD is the optimum power that is supplied to the grid. Now the optimum stator power can be obtained from this curve by using the following equation and is shown by the fig 4.5.

$$P_{sopt} = \frac{P_{opt}}{(1 - s)}$$

Now the optimum stator power curve is as shown below

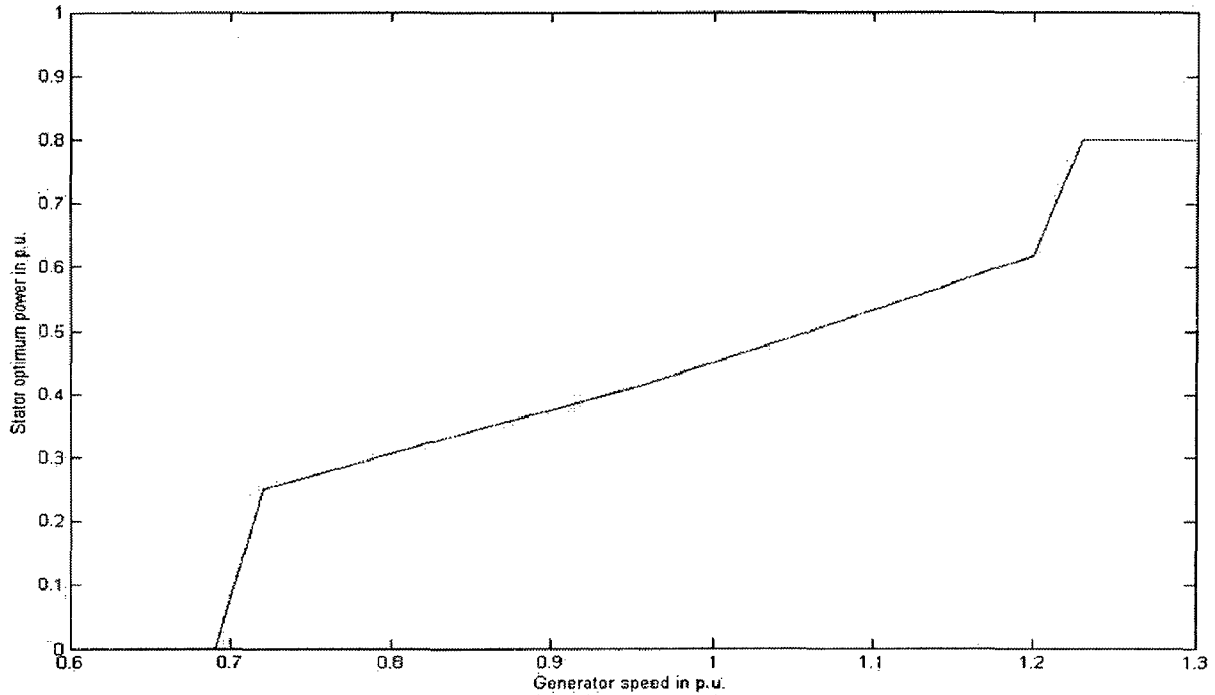


Fig 4.5 Optimum stator power curve

4.4 Pitch angle control:

For higher wind velocities, the turbine energy capture must be limited by applying pitch control. When ever generator speed reaches 1.2 pu, pitch angle control comes into action. Beyond this speed the pitch angle is proportional to the speed deviation from point maximum speed. The complete wind turbine system with pitch angle control and optimum power control is illustrated in the fig 4.6.

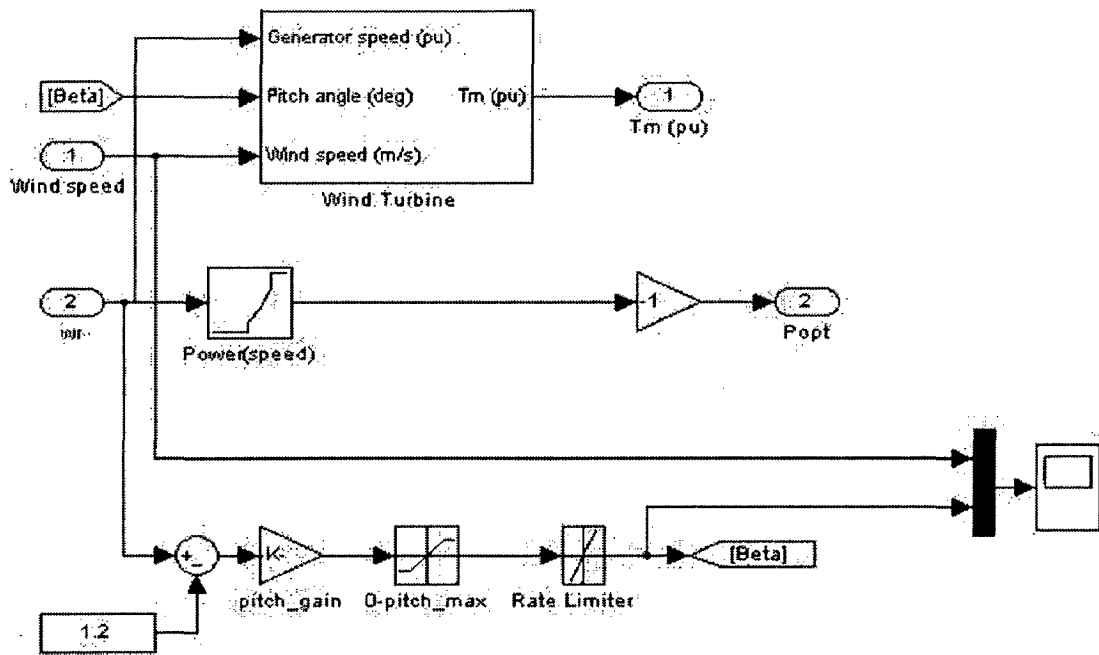


Fig 4.6: The Simulink model of the wind turbine with pitch angle control and Optimum power control

Direct power control of DFIG in wind power applications

5.1 Introduction:

When the direct power control scheme is applied in wind power applications the optimum power control can be achieved. The maximum generator speed can be limited by pitch angle control.

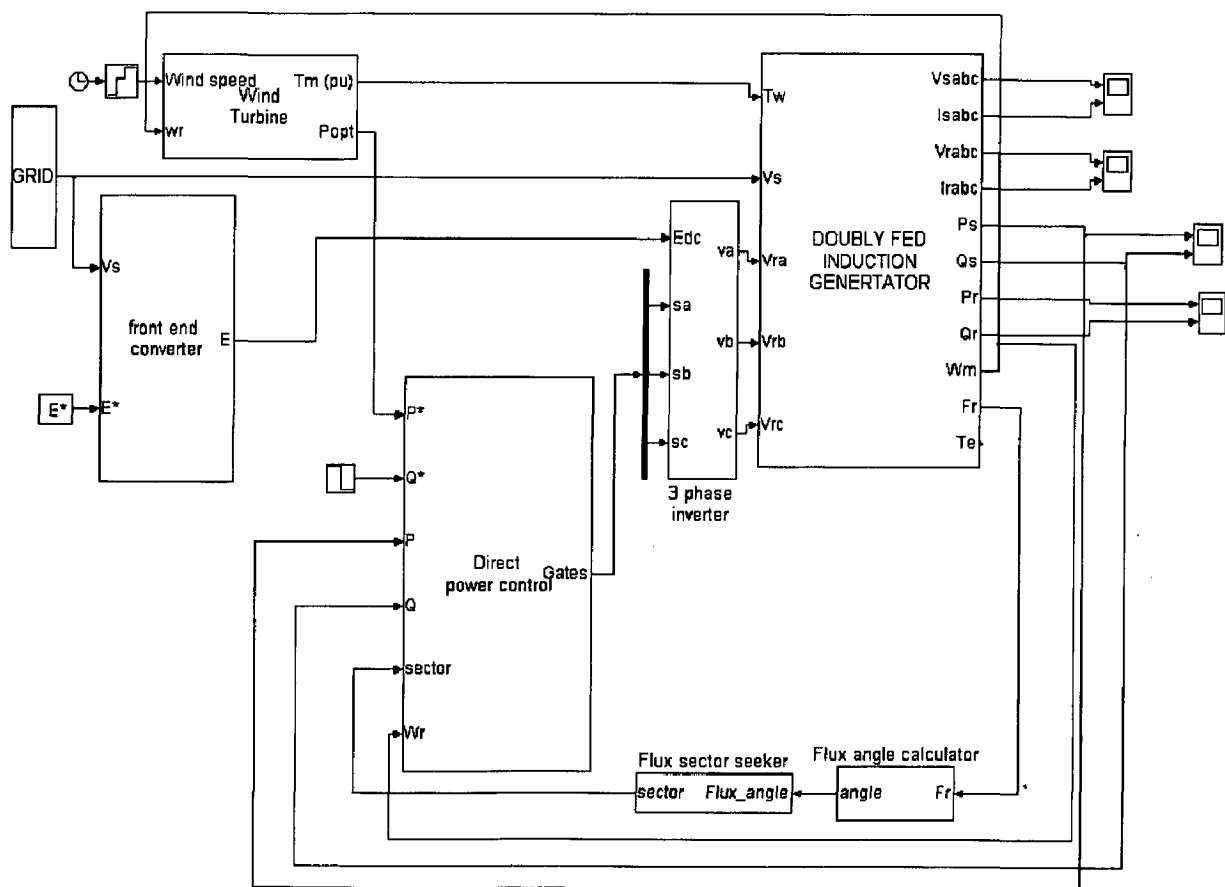


Fig 5.1: Wind power generation by DFIG incorporated with DPC

For the above system input is wind speed. The response of Turbine torque, generator speed, stator current, pitch angle, stator and rotor active powers are observed for change in the wind speed and shown by simulation results.

5.2 Simulation Results:

Response of generator speed, mechanical torque and optimum power with change in wind velocity:

The wind speed is varied in steps and with the variations in wind speed the variation in generator speed, turbine torque and optimum power are shown by the simulation results.

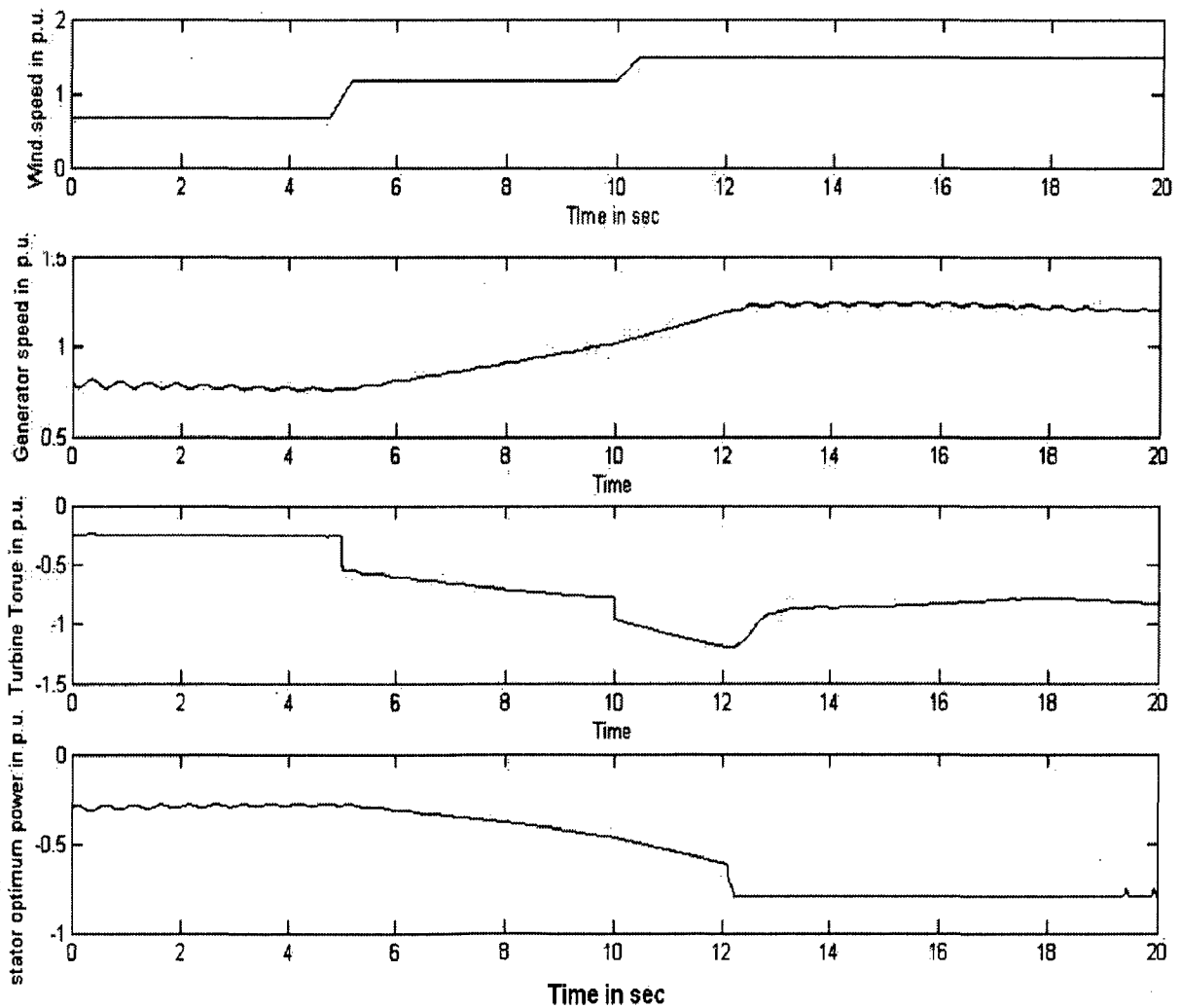


Fig 5.2: Response of generator speed, mechanical torque and optimum power with change in wind velocity

The maximum optimum power is 0.833 p.u. and the maximum generator speed is 1.2 p.u. The system can be operated below and above and at synchronous speeds as shown by the simulation results.

Pitch angle control:

When ever the generator speed reaches the maximum value pitch angle control comes into action and the generator speed is limited to the maximum value. Here in this case maximum speed is 1.2 p.u. The pitch angle control works as shown by the simulation results.

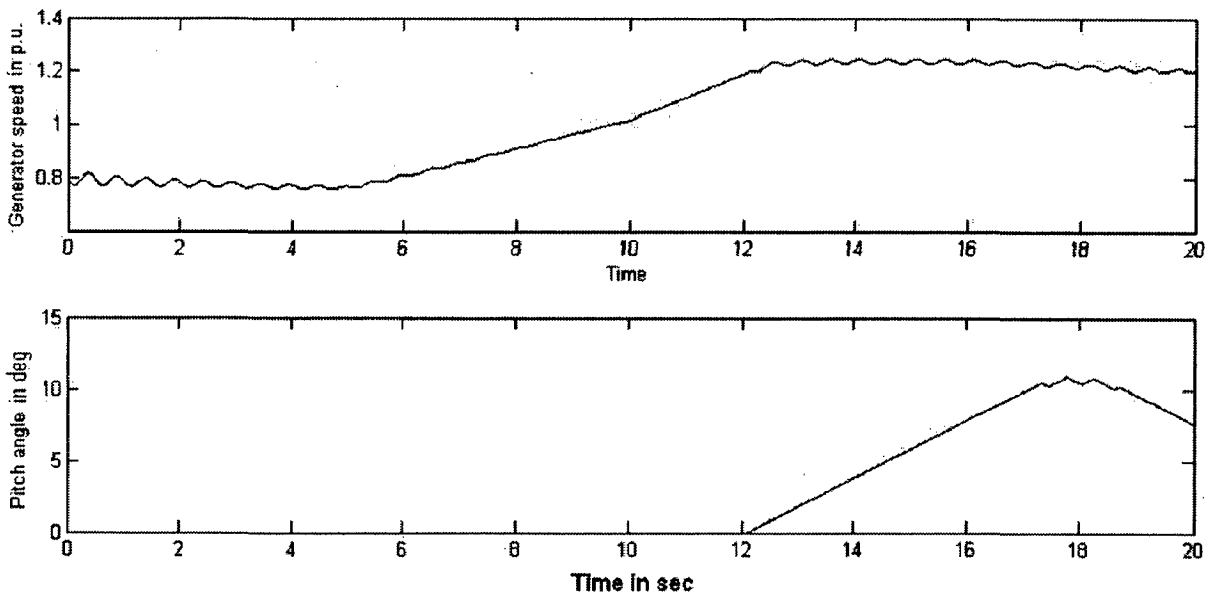


Fig 5.3: Response of speed and pitch angle with change in wind speed

In the Fig 5.3 the generator speed reaches the maximum speed at 12 sec hence the pitch angle control came into action and the generator speed is maintained at the maximum speed.

Response of Stator active power with change in optimum power:

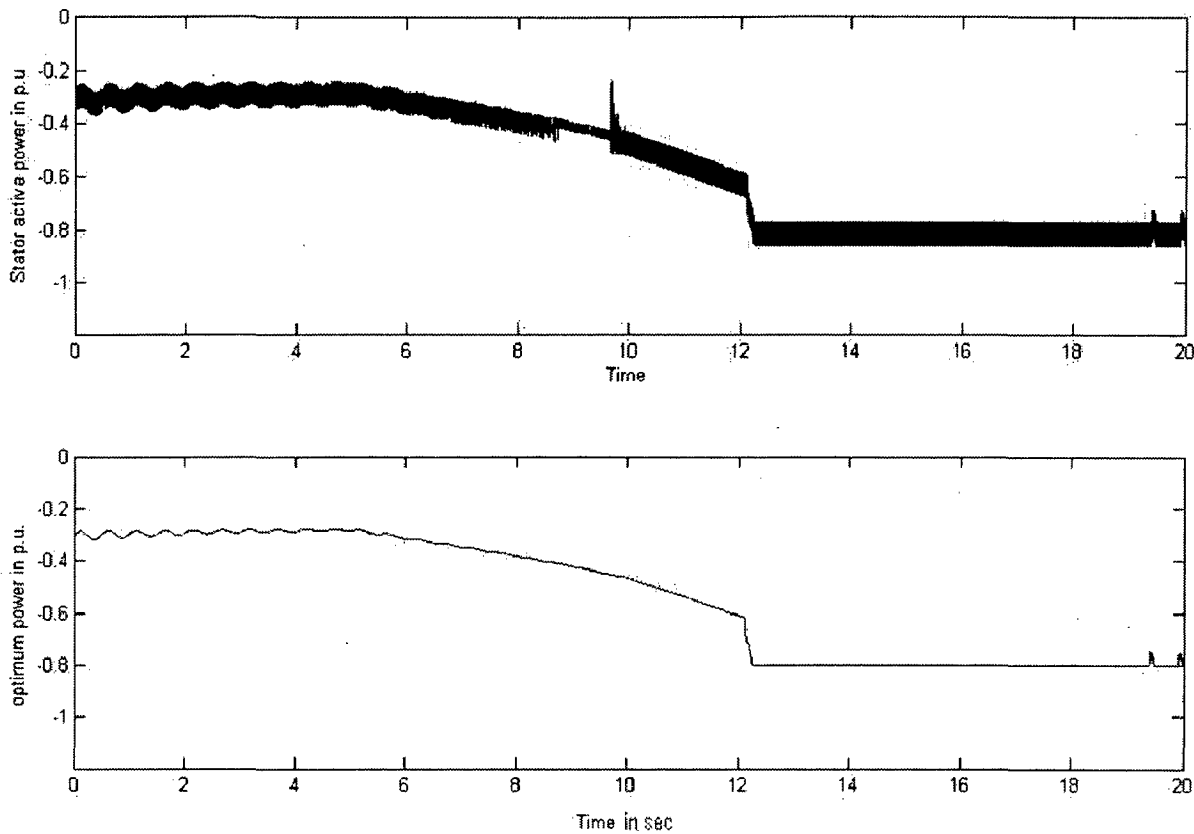


Fig 5.4: Stator active power and Optimum power

When the optimum power is give as the reference stator active power to the control system then the stator active power follows the optimum power with in a band of width P_{band} as shown by the simulation results in fig 5.4. The dynamic response of the system is very good. Hence the optimum power control is achieved by this control system.

Response of Stator current with change in Stator active & reactive powers:

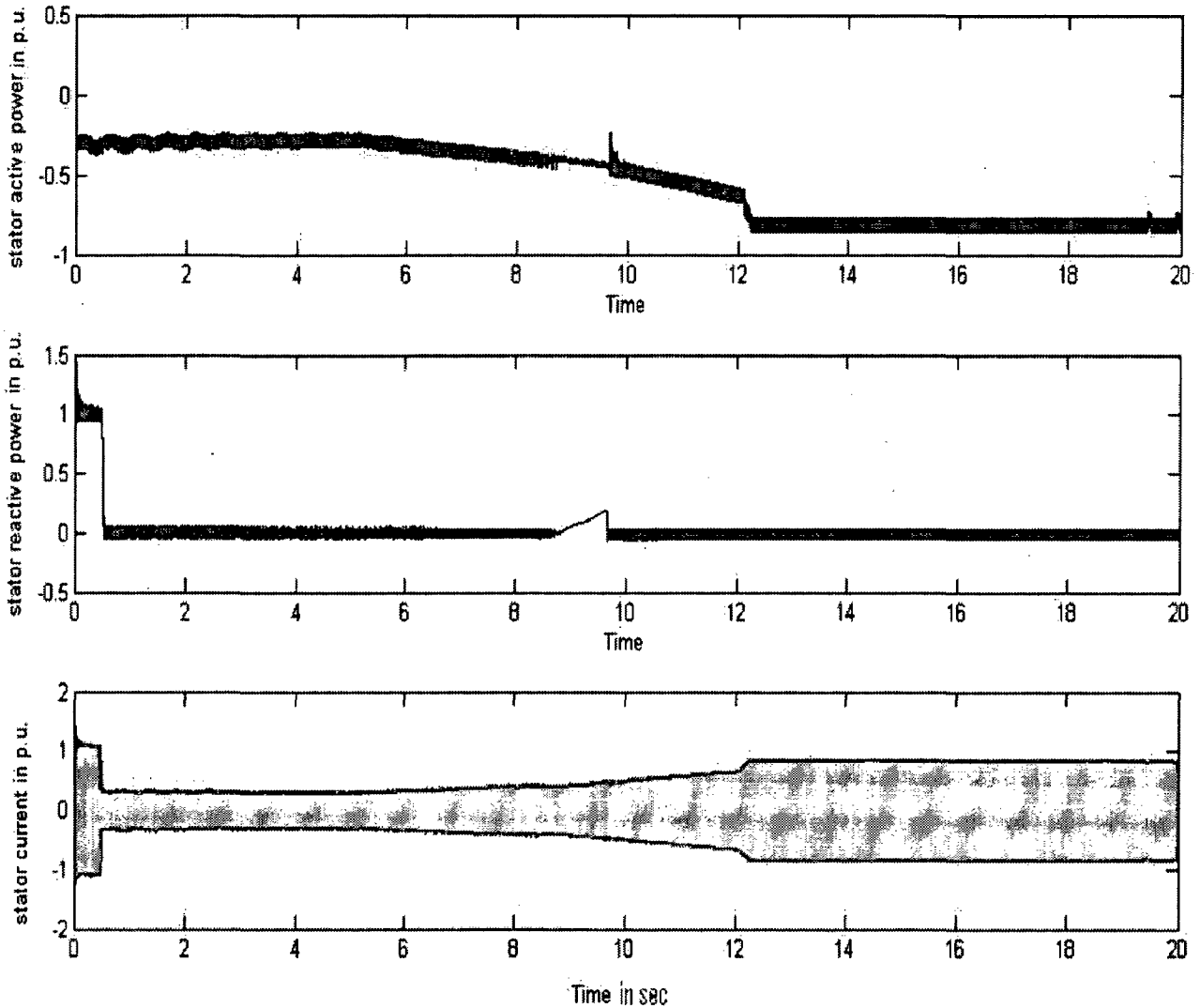


Fig 5.5: Stator active power, reactive power and current

The variation in stator current with change in active and reactive powers is shown in the fig 5.5. The stator reactive power is maintained at zero for maintaining unity power factor on stator side. So the stator KVA is completely the active power generated to the grid. Hence the current is proportional to the stator active power as shown by simulation results.

Rotor active power:

Stator active power of DFIG is always negative that means it always feeds power to the grid. Direction of rotor active power depends upon the speed of the turbine. In the sub-synchronous operation the rotor power is positive i.e. power flows from grid to the rotor circuit and in case of super-synchronous operation power flows from rotor to grid i.e. rotor power is negative. At synchronous speed rotor power is zero. The rotor power is always equal to slip times the stator power.

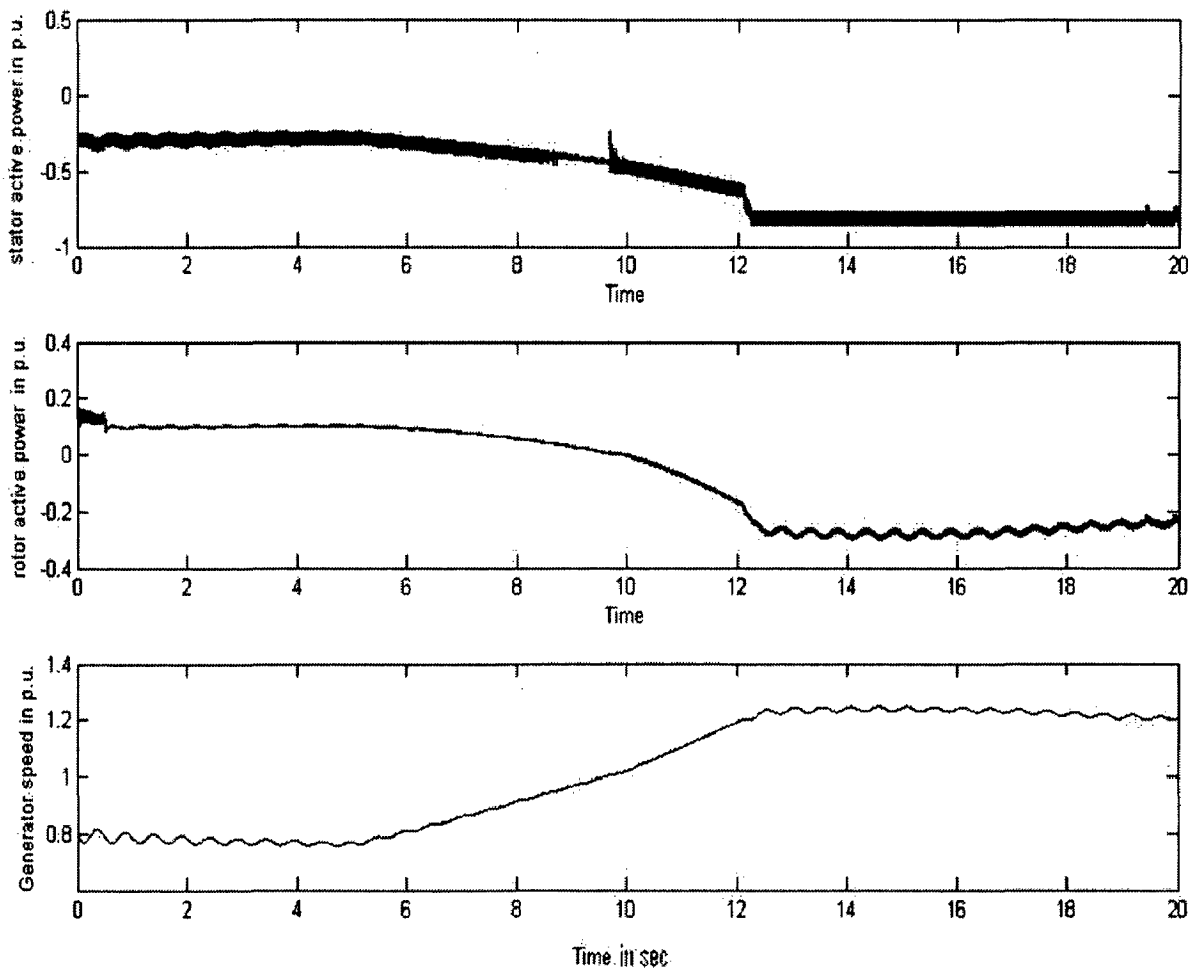


Fig 5.6: Change in Rotor active power with speed



Response of Pitch angle and generator speed for different wind speeds:

There is step change wind speed from 0.67 p.u. to certain value. Then the change in pitch angle and the generator speed are observed. Here for some values of wind speeds the response of the system is shown and from those results we can conclude that up to what speed of wind the system can work satisfactorily.

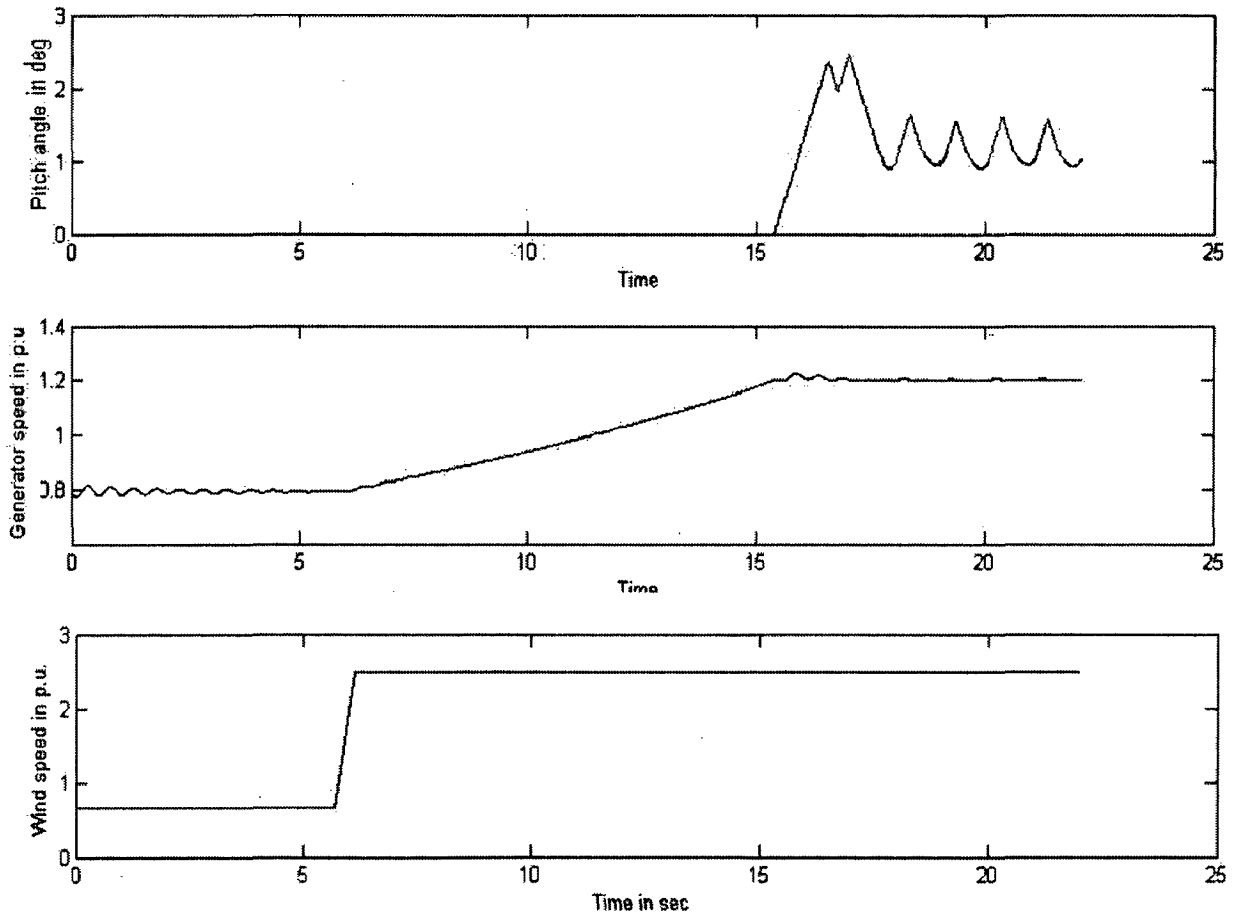


Fig 5.7: pitch angle and generator speed at 2.5 p.u. wind speed

In the above figure wind speed is a step from 0.67 p.u. to 2.5 p.u. The system is working satisfactorily as the turbine speed is limited to 1.2 p.u. By the pitch angle controller. Here the system reached the maximum speed after 15 seconds. For higher speeds of wind the system reaches earlier than this. This can be observed from the simulation results given below.

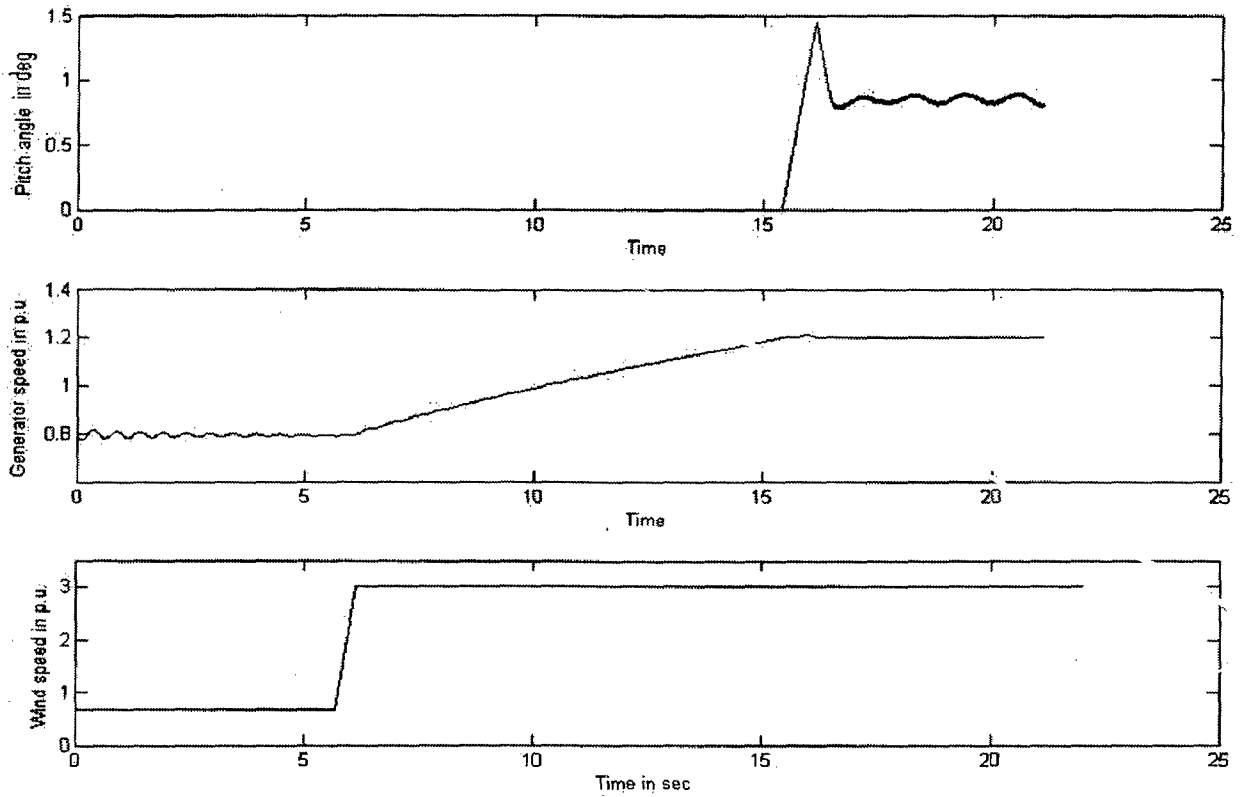


Fig 5.8: pitch angle and generator speed at 3 p.u. wind speed

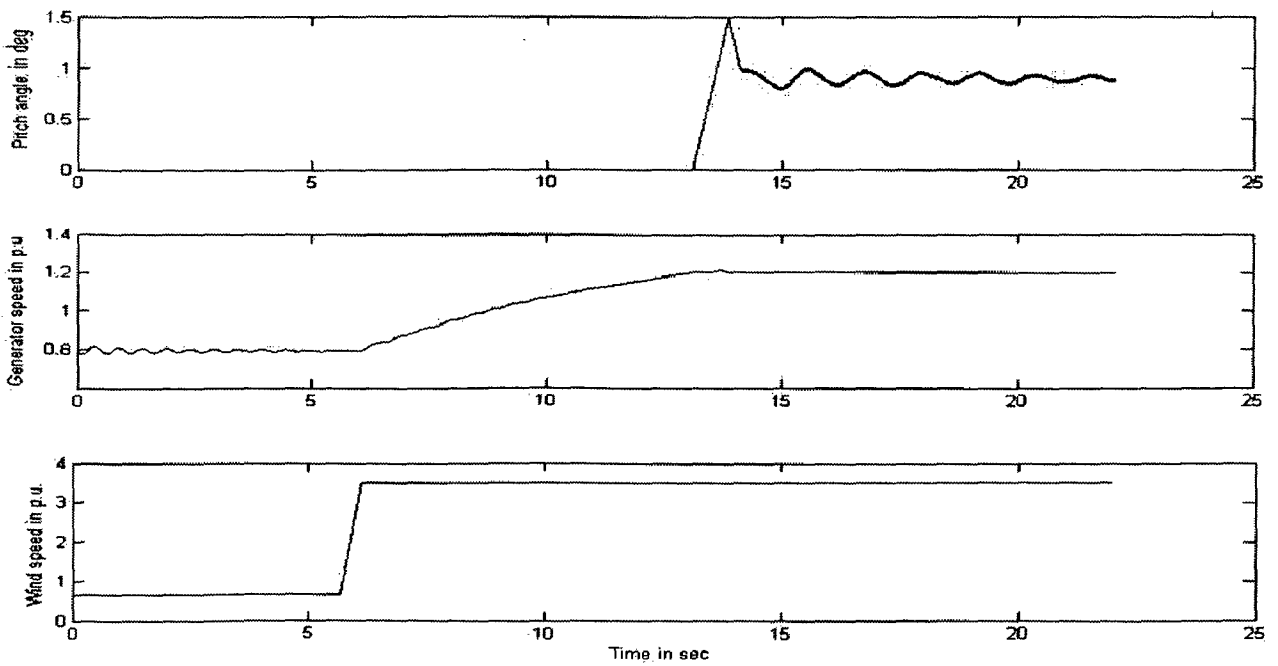


Fig 5.9: pitch angle and generator speed at 3.5 p.u. wind speed

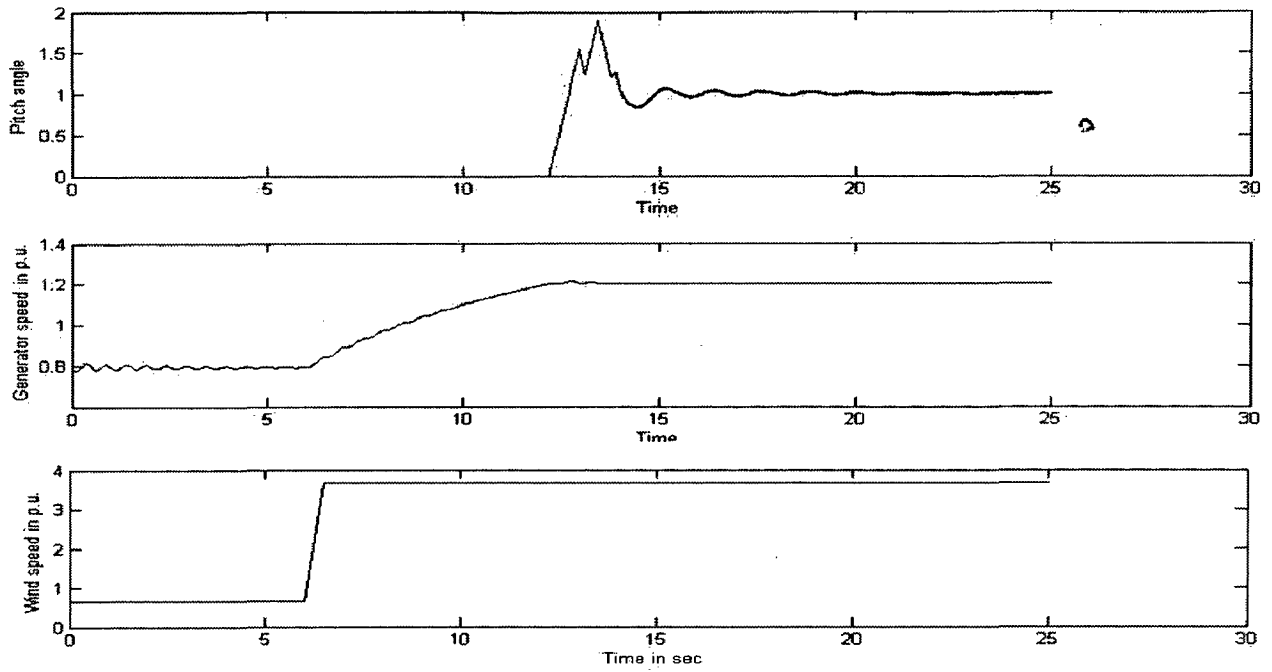


Fig 5.10: pitch angle and generator speed at 3.67 p.u. wind speed

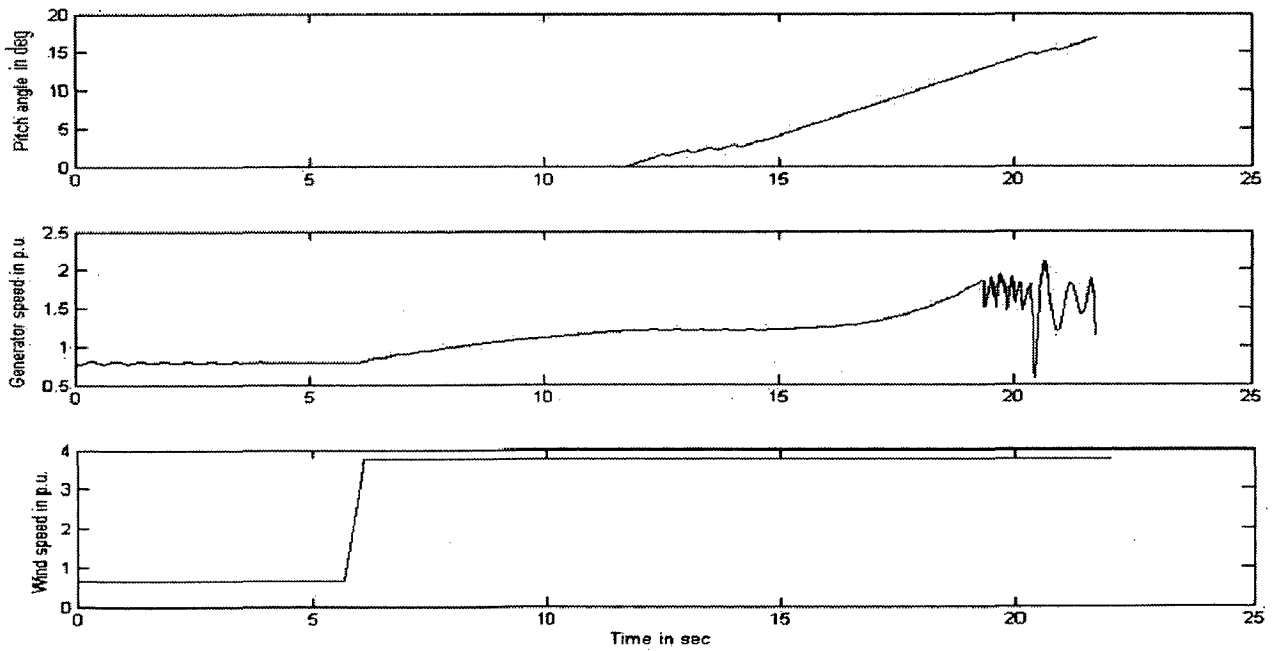


Fig 5.11: pitch angle and generator speed at 3.75 p.u. wind speed

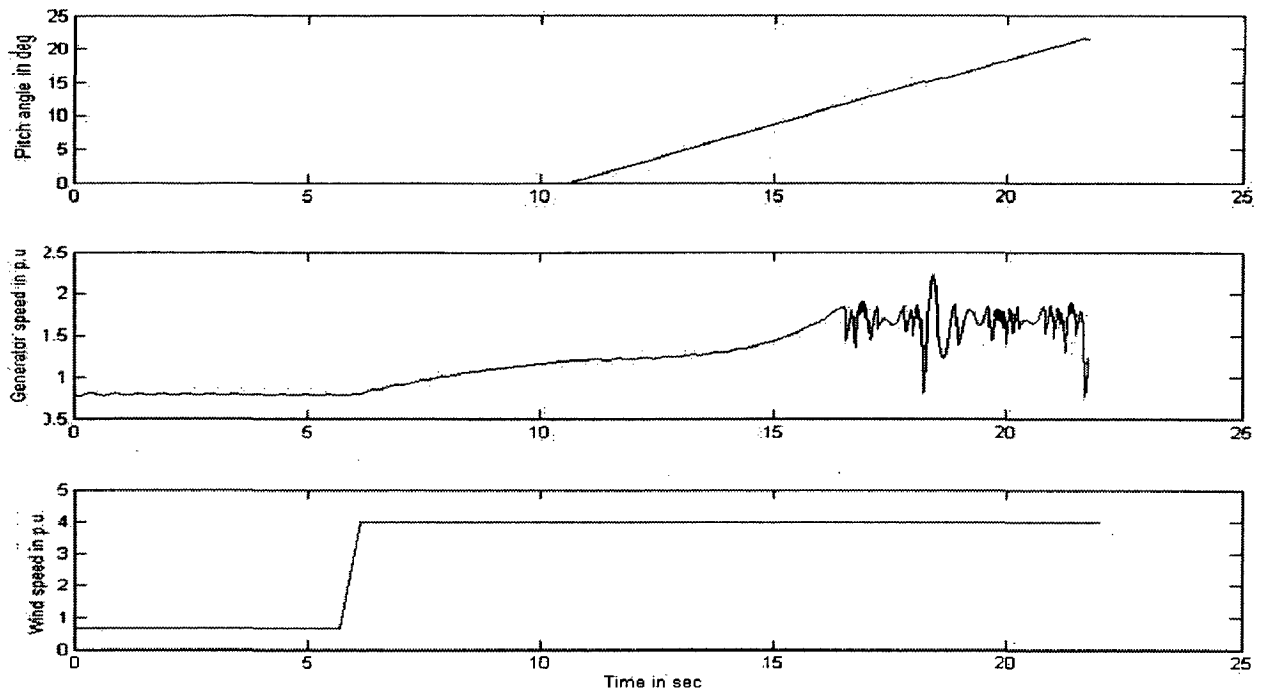


Fig 5.12: pitch angle and generator speed at 4 p.u. wind speed

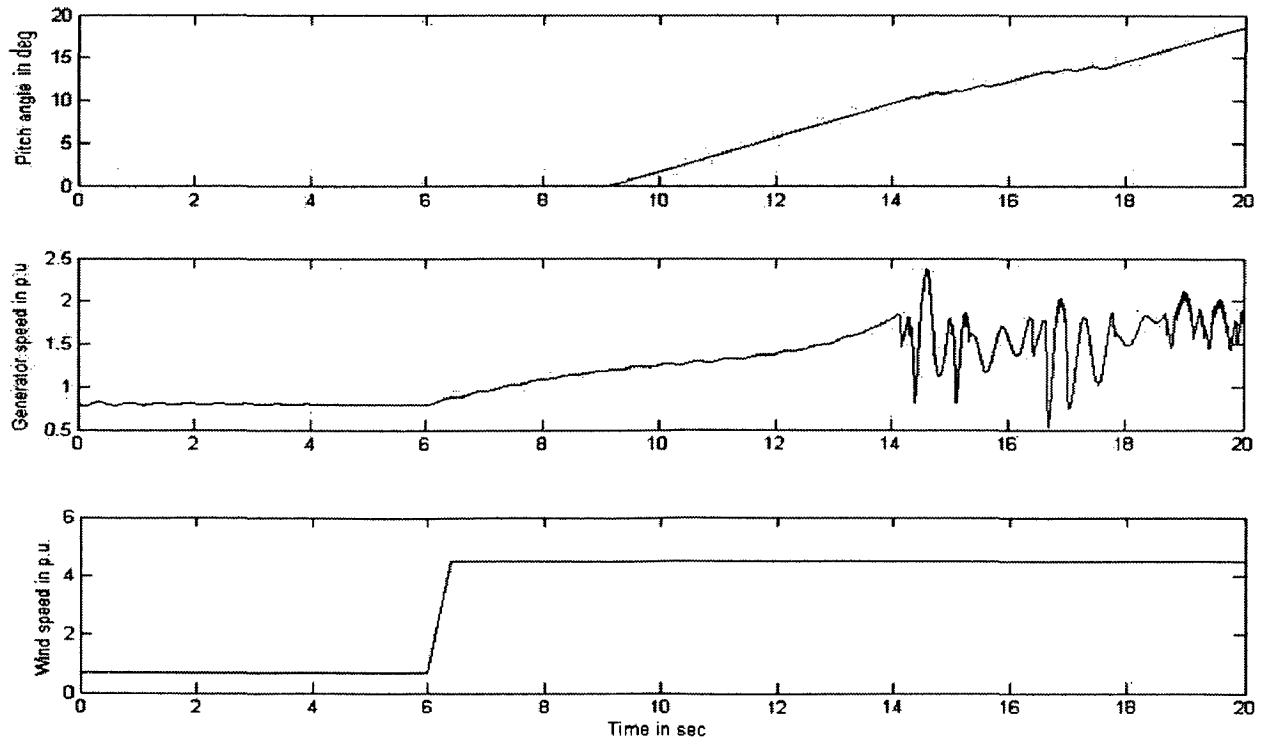


Fig 5.13: pitch angle and generator speed at 4.5 p.u. wind speed

From the simulation results we can conclude that the system can work satisfactorily up to the wind speed of 3.67 p.u. For the wind speeds above this the system fails after small time. If the wind speed is high system fails quickly and vice versa. The pitch angle control comes into action quickly for higher wind speeds.

Efficiency of the generator:

The efficiency of the generator with change in wind speed is as shown in the fig

5.15. For a particular value of wind speed $\%Efficiency = \frac{P_{grid}}{P_{mech}} * 100$ where

P_{grid} is the power supplied to the grid from the machine and given by $P_{grid} = P_s + P_r$ and P_{mech} is the mechanical input to the generator and given by

$$P_{mech} = T_m * \omega_r .$$

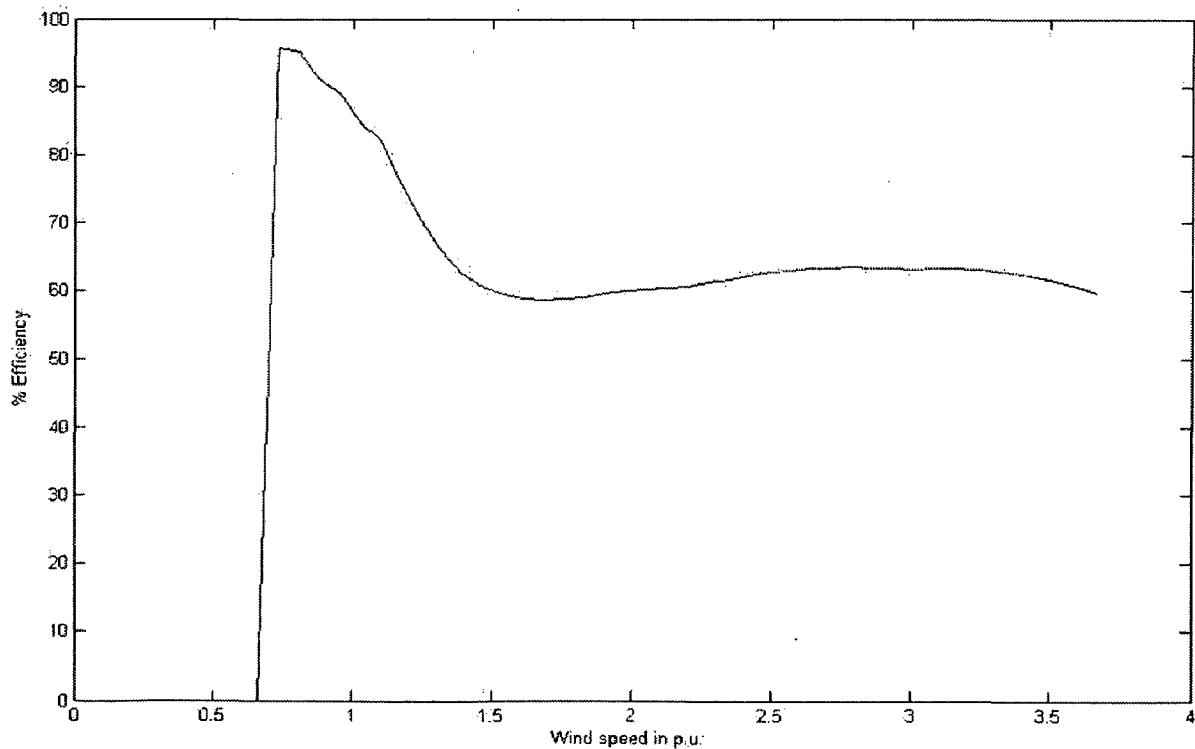


Fig 5.14: Generator efficiency versus wind speed

Conclusions

- ❖ The direct power control of the doubly fed induction generator is capable of controlling the active and reactive powers of a wound rotor induction generator without rotor position sensors.
- ❖ Decoupled control of stator active and reactive power can be obtained and system has good dynamic response as shown by the simulation results. Since it depends only on voltage and current measurements on the stator side, it is insensitive to the parameters of the machine.
- ❖ Direct power control is more advantageous than vector control since the settling time and peak overshoot in case of vector control scheme is higher than that of direct power control scheme.
- ❖ The direct power control of the generator has been embedded in an optimal power controller for maximum energy capture in a wind energy application. Pitch angle control for wind turbine is implemented to limit the generator speed and from the simulation results it is observed that the system works satisfactorily up to 3.67 p.u. of wind speed.

References

- [1] W.Leonhard, Control of Electrical Drives. New York: Springer-Verlag, 1985, ch.13.
- [2] B.K.Bose, "Modern power electronics & Electric drives", Ch-7, pp.329-353.
- [3] Cardici.I. and Ermis M. "Double-output induction generator operating at sub-synchronous and super-synchronous speeds: steady state performance optimization and wind-energy recovery", IEE proc.B, 1992, 139, (S), pp.429-442.
- [4] E.Bogalecka, in Proc.Conf.Rec.EPE Brighton, "Power control of a double fed induction generator with out sensor", vol.8, ch.50, 1993, pp.224–228.
- [5] L.Xu and W.Cheng, "Torque and reactive power control of a doubly fed Induction Machine by position sensorless scheme"IEEE Trans.Ind.Applicat., vol.31, May/June 1995, pp.636–642.
- [6] R.Pena, J.C.Clare and G.M.Asher, "Doubly fed induction generator using back-to-back PWM converters and its application to variable-speed wind-energy generation, Proc.Inst.Elect.Eng" pt. B, vol.143, May 1996, pp. 231–241.
- [7] B.Shanker, S.P.Gupta and P.Agarwal, "Investigation on static slip energy recovery system operated in generating mode", Journal of Institution of Engineers, July 1996, pp. 98-102.
- [8] C.Knowles–Spittle, N.D.Maclsaac and B.A.T.Al Zahawi, "Simulation And Analysis Of 1.4 MW Static Scherbius drive with Sinusoidal Current Converters In Rotor Circuit", Power Electronics and Variable Speed Drives, 21-23 September 1998, Conference Publication No.4560 IEE 1998,pp.617-621.
- [9] R.Datta and V.T.Ranganathan, in Proc.Conf.Rec. 1999 IEEE/IAS Anu.Meeting, 1999 "Decoupled control of active and reactive power for a grid-connected doubly-fed wound rotor induction machine without position sensors", pp. 2623–2630.
- [10] R.Datta and V.T.Ranganathan, "Method for direct control of active and reactive power from the rotor side for a grid connected doubly-fed slip-ring induction machine without position encoder," Indian Patent 797/MAS/99, June 8, 1999.

- [11] S.Muller, M.Deicke and R.W.De Doncker, "Adjustable Speed Generators for Wind Turbines based on Doubly-fed Induction Machines and four Quadrant IGBT Converters Linked to the Rotor", 35th Annual Meeting-IEEE Ind.App.Soc.(IAS), Rome, Italy, Oct.8-12,2000.
- [12] Rajib Datta and V.T.Ranganathan, "Direct Power Control of Grid-Connected Wound Rotor Induction Machine Without Rotor Position Sensors" IEEE Transactions on Power Electronics, Vol. 16, No. 3, MAY 2001,p.p.390-399.
- [13] Zbigniew Krzeminski, in proc.2002 Power conversion conference on "Sensorless Multiscalar Control of Double Fed Machine for Wind Power Generators", Volume1, 2-5 April 2002, pp.334 – 339.
- [14] Rajib Datta and V.T.Ranganathan, "Variable-Speed Wind Power Generation Using Doubly Fed Wound Rotor Induction Machine - A Comparison With Alternative Schemes", IEEE Transactions on Energy Conversion vol.17, NO.3, SEPTEMBER 2002, pp. 414-421.
- [15] S.Muller, M.Deicke and R.W.De Doncker, "Doubly Fed Induction Generator System for Wind Turbines", IEEE Industrial Applications Magazine. May/June 2002, pp. 26-33.
- [16] Arantxa Tapia, Gerardo Tapia et.al, "Modeling and Control of a Wind Turbine Driven Doubly Fed Induction Generator", IEEE Transactions on Energy Conversion vol.18, NO.2, June 2003, pp.194-204.
- [17] Christian Dufour and Jean Belanger, in 35th Annual IEEE Power Electronics Specialists Conference, 2004, "A Real-Time Simulator for Doubly Fed Induction Generator based Wind Turbine Applications", pp.3597-3603.
- [18] Debiprasad Panda, Thomas.A.Lipo, "Double side control of wound rotor induction machine for wind energy application employing half controlled converters", IEEE Transactions on Energy Conversion vol.25,NO.5, June 2005, pp 2468 – 2475.

APPENDIX

Machine details:

A 5hp, 400v, 3 phase, 50 Hz, 4-pole, slip ring induction machine

Parameters of the machine:

Stator resistance = 0.05 p.u.

Rotor resistance = 0.02 p.u.

Stator leakage inductance = 0.1 p.u.

Rotor leakage inductance = 0.1 p.u.

Magnetizing inductance = 5 p.u.

Base values:

Base KVA = 3.75 KVA

Base Voltage = 400 V

Base current = 5.41 A

Base generator speed = 1500 RPM

Base Wind speed = 12 m/s

Front end converter:

Filter resistance = 0.1 Ω

Filter inductance = 12 mH

DC link parameters:

DC link voltage = 450v

Capacitance of DC link Capacitor = 2.4mF